JOC Article

Time-Resolved Resonance Raman Study of the Triplet States of *p*-Hydroxyacetophenone and the *p*-Hydroxyphenacyl Diethyl Phosphate Phototrigger Compound

Chensheng Ma, Peng Zuo, Wai Ming Kwok, Wing Sum Chan, Jovi Tze Wai Kan, Patrick H. Toy, and David Lee Phillips*

Department of Chemistry, The University of Hong Kong, Pokfulam Road, Hong Kong S.A.R., P. R. China

phillips@hku.hk

Received April 21, 2004

Pico- and nanosecond time-resolved resonance Raman (TR^3) spectroscopy have been utilized to study the dynamics and structure of *p*-hydroxyacetophenone (HA) and the *p*-hydroxyphenacyl-caged phototrigger compound *p*-hydroxyphenacyl diethyl phosphate (HPDP) in acetonitrile solution. Transient intermediates were detected and attributed to the triplet states of HA and HPDP. Nanosecond-TR^3 measurements were done for two isotopically substituted HA molecules to help better assign the triplet state carbonyl C═O stretching and the ring related vibrational modes. The dynamics of formation and the spectral characteristics for the triplet states were found to be similar for the HA and HPDP. The temporal evolution at very early picosecond time scale indicates there is rapid intersystem crossing (ISC) conversion and subsequent relaxation of the excess energy of the initially produced energetic triplet state. B3LYP/6-311G** density functional theory (DFT) calculations were done to determine the structures and vibrational frequencies for both the triplet and ground states of HA and HPDP. The calculated spectra reproduce the experimental spectra and the observed isotopic shifts reasonably well and were used to make tentative assignments to all the experimentally observed features. The triplet states were found to have extensive conjugated $\pi\pi^*$ nature with a single-bond-like carbonyl CO bond. We briefly compare the triplet structure and formation dynamics of HA and HPDP as well as the conformational changes upon going from the ground state to the triplet state. We discuss our present results in relation to the initial pathway for the *p*-hydroxyphenacyl photodeprotection process. We also compare and discuss the properties of the HA $\pi\pi^*$ triplet state relative to the published results of other aromatic carbonyl compounds.

Introduction

Photoremovable protecting groups and caged compounds have been receiving increasing interest due to their diverse applications in biochemistry, photolithography, and synthetic organic chemistry.[1−8] The *p*-hydroxyphenacyl group was recently demonstrated to be a new and efficient phototrigger for rapid and localized liberation of various biological stimulants, such as inorganic phosphate,[6,7,9,10] peptides,[8,11] amino acids,[8,11,12] etc. in aqueous solution. The *p*-hydroxyphenacyl cage has been found to possess several superior properties compared to the widely used *o*-nitrobenzyl cage[4,6,13] and newly developed desyl cage systems.[4,6,7,13] Therefore, the *p*-hydroxyphenacyl cage system has been proposed to become the second generation of the α-keto cage type phototriggers.[10] It has been shown that the photodeprotection reaction of *p*-hydroxyphenacyl-caged compounds occurs only in aqueous solution or in solvents containing appreciable water.[6−13] For example, the *p*-hydroxyphenacyl caged phosphate reaction can be described as shown in eq 1.

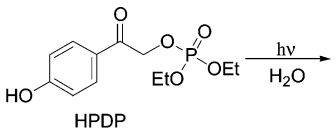

HPDP

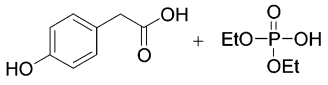

4-hydroxyphenylacetic acid (eq. 1)

By using product analysis, triplet quenchers,[6,10,11] and nano- and picosecond transient absorption,[9,14] several groups have performed mechanistic studies to understand the cleavage and related rearrangement reactions

* To whom correspondence should be addressed. Fax: 852-2857-1586.

(1) Pika, J.; Konosonoks, A.; Robinson, R. M.; Singh, P. N. D.; Gudmundsdottir, A. D. *J. Org. Chem.* **2003**, *68*, 1964−1972.
(2) Pelliccioli, A. P.; Klan, P.; Zabadal, M.; Wirz, J. *J. Am. Chem. Soc.* **2001**, *123*, 7931−7932.
(3) Il′ichev, Y. V.; Schworer, M. A.; Wirz, J. *J. Am. Chem. Soc.* **2004**, *126*, 4581−4595.
(4) Bochet, C. G.. *J. Chem. Soc., Perkin Trans. 1* **2002**, 125−142.
(5) Chan, W. S.; Ma, C.; Kwok, W. M.; Zuo, P.; Phillips, D. L. *J. Phys. Chem. A* **2004**, *108*, 4047−4058.
(6) Park, C.-H.; Givens, R. S. *J. Am. Chem. Soc.* **1997**, *119*, 2453−2463 and references therein.
(7) Givens, R. S.; Athey, P. S.; Matuszewski, B.; Kueper, L. W., III; Xue, J. Y.; Fister, T. *J. Am. Chem. Soc.* **1993**, *115*, 6001−6012 and references therein.
(8) Givens, R. S.; Weber, J. F. W.; Conrad, P. G.; Orosz, G.; Donahue, S. L.; Thayer, S. A. *J. Am. Chem. Soc.* **2000**, *122*, 2687−2697 and references therein.

10.1021/jo049331a CCC: $27.50
Published on Web 09/09/2004

of the *p*-hydroxyphenacyl photodeprotection processes. Different mechanisms have been proposed, and there remain conflicting interpretations and controversies about the photophysical and photochemical pathways of these processes. The divergences in these previous studies revolve mainly about two issues: the multiplicity and the primary photochemical step of the photorelease mechanism. Givens, Wirz, and co-workers suggested that the lowest triplet state is the precursor to the chemical pathway, and they favor a cleavage mechanism involving direct release of the leaving group from the excited triplet state.[6,9−11] On the other hand, Wan and co-workers reported a singlet mechanism and proposed that the primary step responsible for the photochemistry is the single excited state intramolecular proton transfer (ESIPT) from the phenolic proton to the ketone carbonyl oxygen mediated by water solvent.[14] In addition, work by Falvey and co-workers on phenacyl esters lacking the *p*-hydroxy group appears to indirectly support the triplet mechanism. Falvey and co-workers observed that hydrogen abstraction from the solvent by the triplet carbonyl oxygen to form the ketyl radical is the initial step for the photocleavage reaction.[14] The origin of the photolability of the *p*-hydroxyphenacyl chromophore is still not well understood, and further work is needed to better address the overall photoexcited reaction pathways and to clearly identify the reactive intermediate so as to clarify the validity of the possible reaction mechanisms suggested thus far.

Information about the triplet structure of the *p*-hydroxyphencyl-caged compounds and their intersystem crossing (ISC) rate of the singlet to triplet conversion are among the key experimental pieces of information needed to establish the photodeprotection mechanism and clarify the related ambiguity in the reaction pathways. Based on time-resolved measurements employing the pico- and nanosecond transient absorption techniques, the triplet lifetime and tentative identification of several possible transient species have been reported for a couple of *p*-hydrophencyl compounds and the parent compound *p*-hydroxyacetophenone (HA).[9,14] However, the broad structureless absorption spectra provide little structural data for the triplet state and other possible intermediates. Direct information on early time photophysical and photochemical dynamics occurring immediately after photoexcitation is still lacking due to the limited time resolution of most previous experiments. Time-resolved vibrational spectroscopy measurement with pico- or even femtosecond time resolution[16] should provide more insight into the structure and dynamics of formation of the intermediates previously observed in the transient absorption studies.[9,14] Here, we report pico- and nanosecond time-resolved resonance Raman (TR^3) results for the *p*-hydroxyphenacyl caged phosphate compound, the *p*-hydroxyphenacyl diethyl phosphate (HPDP), and the parent compound HA. Structures of the two compounds are as follows.

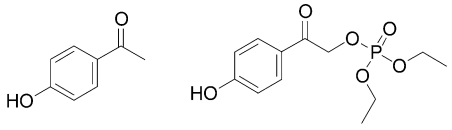

HA HPDP

From these spectra, we elucidate the structure as well as the formation and decay kinetics of the triplet states for HPDP and HA. These results provide additional insight to differentiate the triplet vs singlet reaction mechanisms previously proposed by other groups.

Besides their intriguing applications as photoprotecting group for biological stimulants, which is one of the major reasons for the present investigation, the importance of the photochemistry and triplet state properties for the two compounds render the time-resolved vibrational spectroscopic results of this work interesting in their own right. The two molecules studied here belong to substituted aromatic carbonyl compounds, and it is well-known that the triplet states of these kinds of compounds are important reactive intermediates in a wide variety of photochemical reactions.[17−24] Extensive work has been reported in the literature to characterize the triplet states and to correlate these properties with their reactivity.[17,18−22,25−30,31−33] Some time-resolved vibrational studies using both the TR^3 [34−37] and time-resolved IR (TRIR)[38−40] spectroscopy have been done to investigate the possible correlation between the triplet structure, especially the frequency of the triplet carbonyl C═O stretching vibration, with the $^3n\pi^*$ and $^3\pi\pi^*$ electronic configurations and the triplet reactivity. Some interesting trends have been reported. However, the compounds studied previously are those with typical lowest $^3n\pi^*$ or $^3\pi\pi^*$ state, or say well-separated $^3n\pi^*$ and $^3\pi\pi^*$ configurations. Further time-resolved vibrational studies are needed to seek a more general correlation

(9) Conrad, P. G., II; Givens, R. S.; Hellrung, B.; Rajesh, C. S.; Ramseier, M.; Wirz, J. *J. Am. Chem. Soc.* **2000**, *122*, 9346−9347.
(10) Givens, R. S.; Park, C. H. *Tetrahedron Lett.* **1996**, *37*, 6259−6262.
(11) Givens, R. S.; Jung, A.; Park, C. H.; Weber, J.; Bartlett, W. *J. Am. Chem. Soc.* **1997**, *119*, 8369−8370.
(12) Conrad, P. G., II; Givens, R. S.; Weber, J. F. W.; Kandler, K. *Org. Lett.* **2000**, *2*, 1545−1547.
(13) Givens, R. S.; Kueper, L. W. *Chem. Rev.* **1993**, *93*, 55−66.
(14) (a) Brousmiche, D. W.; Wan, P. *J. Photochem. Photobiol., A* **2000**, *130*, 113−118. (b) Zhang, K.; Corrie, J. E. T.; Munasinghe, R. N.; Wan, P. *J. Am. Chem. Soc.* **1999**, *121*, 5625−5632.
(15) Banerjee, A.; Falvey, D. E.; *J. Am. Chem. Soc.* **1998**, *120*, 2965−2966.
(16) Ma, C.; Chan, W. S.; Kwok, W. M.; Zuo, P.; Phillips, D. L. *J. Phys. Chem. B* **2004**, *108*, 9264−9276.
(17) (a) Wagner, P. J.; Hammond, G.. S. *J. Am. Chem. Soc.* **1965**, *87*, 4009−4011. (b) Wagner, P. J.; Kemppainen, A. E. *J. Am. Chem. Soc.* **1968**, *90*, 5898−5899. (c) Wagner, P. J.; Kemppainen, A. E.; Schott, H. N. *J. Am. Chem. Soc.* **1973**, *95*, 5604−5614. (d) Wagner, P. J.; Truman, R. J.; Scaiano, J. C. *J. Am. Chem. Soc.* **1985**, *107*, 7093−7097.
(18) Schwartz, B. J.; Peteanu, L. A.; Harris, C. B. *J. Phys. Chem.* **1992**, *96*, 3591−3598.
(19) (a) Webb, S. P.; Phillips, L. A.; Yeh, S. W.; Tolbert, L. M.; Clark, J. H. *J. Phys. Chem.* **1996**, *90*, 5154−5164. (b) Webb. S. P.; Yeh, S. W.; Phillips. L. A.; Tolbert, M. A.; Clark, J. H. *J. Am. Chem. Soc.* **1984**, *106*, 7286−7288.
(20) (a) Yang, N. C.; McClure, D. S.; Murov, S. L.; Houser, J. J.; Dusenbery, R. *J. Am. Chem. Soc.* **1967**, *89*, 5466−5468. (b) Yang, N. C.; Dusenbery, R. L. *J. Am. Chem. Soc.* **1968**, *90*, 5899−5900. (c) Yang, N. C.; Kimura, M.; Eisenhardt, W. *J. Am. Chem. Soc.* **1973**, *95*, 5058−5060.
(21) Baum. E. J.; Wan, J. K. S.; Pitts, J. N. *J. Am. Chem. Soc.* **1966**, *88*, 2652−2659.
(22) Rauh, R. D.; Leermakers, P. A. *J. Am. Chem. Soc.* **1968**, *90*, 2246−2249.
(23) Matsushita, Y.; Yamaguchi, Y.; Hikida, T. *Chem. Phys.* **1996**, *213*, 413−419.
(24) Colley, C. S.; Grills, D. C.; Besley, N. A.; Jockusch, S.; Matousek, P.; Parker, A. W.; Towrie, M.; Turro, N. J.; Gill, P. M. W.; George, M. W. *J. Am. Chem. Soc.* **2002**, *124*, 14952−14958.

between the triplet structure−electronic configuration−reactivity for the wide range of aromatic carbonyls, especially those with close-lying $^3n\pi^*$ and $^3\pi\pi^*$ states, whose structural studies remain very scarce in the literature. The *p*-hydroxyphenacyl caged compounds studied here and many other derivatives of acetophenone have nearly degenerate $^3n\pi^*$ and $^3\pi\pi^*$ configurations.[17,20,22,28−31,41−43] It is possible that, due to the strongly mixed character of the two configurations, the triplets of these compounds could be substantially different from those of the typical well-separated $^3n\pi^*$ or $^3\pi\pi^*$ states. The spectra reported in this paper are therefore expected to contribute to a better understanding to the triplet states of derivatives of acetophenone that have nearly degenerate $^3n\pi^*$ and $^3\pi\pi^*$ configurations.

The TR^3 spectra presented here were acquired with 266 nm excitation and 400 (ps-TR^3) or 416 nm (ns-TR^3) probe wavelength in acetonitrile solvent. The ISC rate was estimated on the basis of the early picosecond temporal evolution of the triplet state spectra, and the lifetime of the triplet state was obtained from the spectral decay up to 400 ns. For HA, the TR^3 measurements have also been done to the carbonyl carbon isotopic-substituted (HA-^{13}C) and ring-deuterated (HA-D_4) compounds shown below to help assign the triplet state carbonyl C═O stretching and the ring-related vibrational modes.

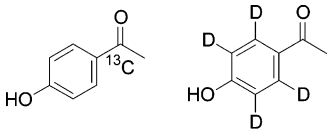

HA-^{13}C HA-D_4

To help determine the triplet-state geometry, vibrational frequencies, and to make assignments to the experimental vibrational bands, density functional theory (DFT) calculations were also done employing the B3LYP method with a 6−311 G** basis set for both the ground and triplet states of the two compounds. The early time dynamics, the comparison of the triplet-state structures between the parent HA and caged HPDP compounds, and a comparison of the triplet-state structure to that of the corresponding ground state allow us to comment on the present controversy over the initial stages of the phenacyl deprotection mechanism and related processes. We also discuss briefly our results in relation to the nature of the triplet state and make comparisons to those reported previously in the literature.

Experimental and Computational Methods

FT-IR spectra of the compounds studied were recorded using a FT-IR spectrometer with the sample encased in solid KBr windows. A normal Raman spectrum of the solid phase HP was obtained using a Raman microspectrometer employing 514 nm excitation from an Ar ion laser. The spectral resolution of these spectrometers were approximately 5 cm^{-1} for both the Raman and IR spectra.

The ps-TR^3 experiments were performed using a newly developed ultrafast laser system in this laboratory that has been described elsewhere.[16,44] Briefly, the pump and probe wavelengths were 267 and 400 nm with ∼15 and 8 μJ/pulse energy, respectively, ∼1 ps pulse length, and ∼15 cm^{-1} line width. The time resolution of the system is ∼2 ps, and the time delay between the pump and probe pulses was changed using an optical delay line. The laser beams were loosely focused (∼250 and 150 μm for the pump and probe beam, respectively) onto a thin film stream (thickness ∼500 μm) of a recirculated acetonitrile solution with sample concentration of ∼1 mM. The Raman light was collected in a back-scattering configuration and detected by a liquid-nitrogen-cooled CCD detector.

The ns-TR^3 measurements were done using an experimental apparatus described previously.[45−47] The pump wavelength was 266 nm, and the 416 nm probe wavelength came from the first Stokes of a hydrogen Raman shifted line pumped by the third harmonic (355 nm) from the second Nd:YAG laser. The time delay between the pump and probe beam was controlled electronically by a pulse generator, and the time resolution of these experiments was ∼10 ns. The energy of the pump and probe pulses was in the 2−2.5 mJ range with a repetition rate of 10 Hz. The arrangements for the sample and Raman signal detection are similar to those used in the picosecond experiments. To check the quenching effect by oxygen, the measurements were performed under open air as well as under nitrogen and with oxygen being bubbled through the sample system.

For both the ps- and ns-TR^3 experiments, the spectra presented were obtained from subtraction of an appropriately scaled probe-before-pump spectrum from the corresponding

(25) Hirota, N. *Chem. Phys. Lett.* **1969**, *4*, 305−308.
(26) Cheng, T. H.; Hirota, N. *Chem. Phys. Lett.* **1972**, *13*, 194−198.
(27) Mao, S. W.; Wong, T. C.; Hirota, N. *Chem. Phys. Lett.* **1972**, *13*, 199−204.
(28) (a) Lutz, H.; Duval, M. C.; Bréhéretm. E.; Lindzvist, L. *J. Phys. Chem.* **1972**, *76*, 821−822. (b) Lutz, H.; Bréhéretm, E.; Lindqvist, L. *J. Phys. Chem.* **1973**, *77*, 1758−1762.
(29) (a) Lim, E. C.; Li, Y. H.; Li, R. *J. Chem. Phys.* **1970**, *53*, 2443−2448. (b) Li, Y. H.; Lim, E. C. *Chem. Phys. Lett.* **1970**, *7*, 15−18.
(30) Koyanagi, M. Zwarich, R. J.; Goodman, L. *J. Chem. Phys.* **1972**, *56*, 3044−3060.
(31) Ohmori, N.; Suzuki, T.; Ito, M. *J. Phys. Chem.* **1988**, *92*, 1086−1093.
(32) Dym. S.; Hochstrasser, R. M. *J. Chem. Phys.* **1969**, *51*, 2458−2468.
(33) (a) Case, W. L.; Kearns, D. R. *J. Chem. Phys.* **1970**, *52*, 2175−2191. (b) Kearns, D. R.; Case, W. A. *J. Am. Chem. Soc.* **1966**, *88*, 5087−5097.
(34) Tahara, T.; Hamaguchi, H.; Tasumi, M. *J. Phys. Chem.* **1990**, *94*, 170−178.
(35) Tahara, T.; Hamaguchi, H.; Tasumi, M. *J. Phys. Chem.* **1987**, *91*, 5875−5880.
(36) Tahara, T.; Hamaguchi, H.; Tasumi, M. *Chem. Phys. Lett.* **1988**, *152*, 135−139.
(37) Eijk, A. M. J. v.; Verhey, P. F. A.; Huizer, A. H.; Varma, C. A. G. O. *J. Am. Chem. Soc.* **1987**, *109*, 6635−6641.
(38) Tanaka, S.; Kato, C.; Horie, K.; Hamaguchi, H. *Chem. Phys. Lett.* **2003**, *381*, 385−391.
(39) Srivastava, S.; Yourd, E.; Toscano, J. P. *J. Am. Chem. Soc.* **1998**, *120*, 6173−6174.
(40) Sun, H, Frei, H. *J. Phys. Chem. B* **1997**, *101*, 205−209.
(41) Shailaja, J.; Lakshminarasimhan, P. H.; Pradhan, A. R.; Sunoj, R. B.; Jockusch, S.; Karthikeyan, S.; Uppili, S.; Chandrasekhar, J.; Turro, N. J.; Ramamurthy, V. *J. Phys. Chem. A* **2003**, *107*, 3187−3198.
(42) Rusakowicz, R.; Byers, G. W.; Leermakers, P. A. *J. Am. Chem. Soc.* **1971**, *93*, 3263−3266.
(43) Warren, J. A.; Bernstein, E. R. *J. Chem. Phys.* **1986**, *85*, 2365−2367.
(44) Kwok, W. M.; Zhao, C.; Li, Y.-L.; Guan, X.; Wang, D.; Phillips, D. L. *J. Am. Chem. Soc.* **2004**, *126*, 3119−3131.
(45) (a) Kwok, W. M.; Phillips, D. L. *J. Chem. Phys.* **1996**, *104*, 2529−2540. (b) Kwok, W. M.; Phillips, D. L. *J. Chem. Phys.* **1996**, *104*, 9816−9832. (c) Man, S. Q.; Kwok, W. M.; Johnson, A. E.; Phillips, D. L. *J. Chem. Phys.* **1996**, *105*, 5842−5857.
(46) (a) Pan, D.; Phillips, D. L. *J. Phys. Chem. A* **1999**, *103*, 4737−4743. (b) Zheng, X.; Phillips, D. L. *J. Phys. Chem. A* **2000**, *104*, 6880−6886. (c) Zhu, P.; Ong, S. Y.; Chan, P. Y.; Leung, K. H.; Phillips, D. L. *J. Am. Chem. Soc.* **2001**, *123*, 2645−2649.
(47) (a) Li, Y.-L.; Leung, K. H.; Phillips, D. L. *J. Phys. Chem. A* **2001**, *105*, 10621−10625. (b) Li, Y.-L.; Chen, D.-M.; Phillips, D. L. *J. Org. Chem.* **2002**, *67*, 4228−4235. (c) Li, Y.-L.; Wang, D.; Phillips, D. L. *J. Chem. Phys.* **2002**, *117*, 7931−7941. (d) Ong, S. Y.; Chan, P. Y.; Zhu, P.; Leung, K. H.; Phillips, D. L. *J. Phys. Chem. A* **2003**, *107*, 3858−3865.

pump−probe spectrum. Acetonitrile solvent Raman bands were used to calibrate the TR^3 spectra with an estimated accuracy of ± 5 cm^{-1} in absolute frequency.

HPDP was synthesized following the method suggested in refs 48 and 49. The compound was characterized as follows. ^1H NMR (400 MHz, $CDCl_3$) δ: 1.41 (t, $J = 7.0$ Hz, 6H), 4.28 (m, $J = 7.3$ Hz, 4H), 5.17 (d, $J = 11.7$ Hz, 2H), 6.79 (d, $J = 8.7$ Hz, 2H), 7.51 (d, $J = 8.7$ Hz, 2H), 7.57 (d, $J = 9.2$ Hz, 2H), 9.08 (s, 1H). ^{13}C NMR (100 MHz, CDC_{l3}) δ: 16.1, 64.9, 68.8 (2C), 115.9 (2C), 125.5, 130.0 (2C), 162.6, 189.9. MS(EI) (*m*/*z*) 288 [$C_{12}H_{17}PO_6^+$]. UV (CH_3CN) $\lambda_{max} = 275$ nm. HA-^{13}C and HA-D_4 were synthesized using the method suggested in ref 50. These compounds were characterized as follows. For HA-^{13}C: ^1H NMR (400 MHz, $CDCl_3$) δ: 2.56 (d, $J = 8.0$ Hz, 3H), 5.45 (s, H), 6.89 (d, $J = 12$ Hz, 2H), 7.92 (d, $J = 12$ Hz, 2H). ^{13}C NMR (100 MHz, CDC_{l3}) δ: 179.2 (the carbonyl ^{13}C). MS (EI) (*m*/*z*): 137 [$C_7{}^{13}CH_8O_2^+$], 122 [$C_6{}^{13}CH_5O_2^+$], 93 [$C_6H_5O^+$]. For HA-D_4: ^1H NMR (400 MHz, $CDCl_3$) δ: 2.17 (3H), 5.59 (s, H). The identity of the samples were further confirmed by vibrational analysis of their FTIR spectra as given below. Normal HA is available commercially and was used after recrystallization. Spectroscopic grade acetonitrile solvent was used as received for the TR^3 measurements. UV absorption measurements before and after sample use revealed no appreciable degradation for samples used in both the ns- and ps-TR^3 experiments.

The optimized geometry, vibrational mode, and frequencies for the ground-state HPDP and HA were obtained from B3LYP density functional theory (DFT) calculations employing a 6-311G** basis set. The open-shell UB3LYP method with the same basis set was used for the triplet computations. No imaginary frequency mode was observed for any of the optimized structures. The DFT Raman and IR activities were also calculated to allow direct comparison with the experimental spectra. Frequency calculations were also done for the triplet and ground states of HA-^{13}C, HA-D_4, and carbonyl oxygen isotopic substituted HA-^{18}O. The spin densities were obtained from the triplet calculations, and no appreciable spin contamination was found. All the calculations were done using the Gaussian 98 program suite.[51]

Results and Discussion

A. Optimized Structure and Vibrational Analysis of the Ground State of HA and HPDP. Parts a and b of Figure 1 display the optimized geometry found from the B3LYP/6-311G** calculations for the HA and HPDP ground states, respectively. Selected structural parameters and calculated total energy including the zero-point energy are given in Table 1 for (a) HA and (b) HPDP. A full list of the optimized geometry parameters and their computed total energy can be found in the Supporting Information. The X-ray diffraction data of crystallized

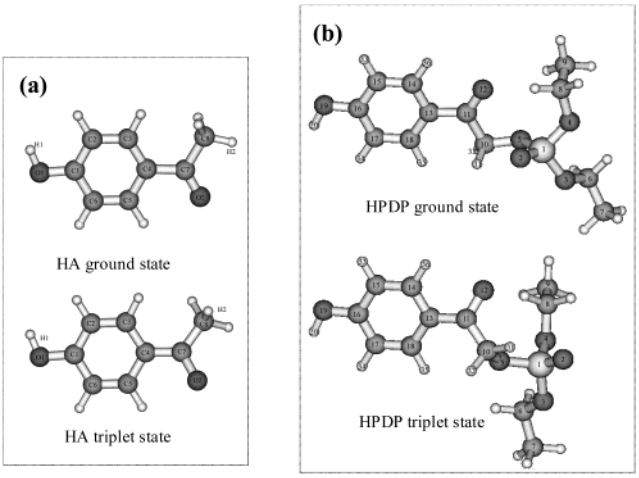

FIGURE 1. Optimized structures for the ground and triplet states of (a) HA and (b) HPDP computed from DFT calculations using B3LYP (ground) and UB3LYP (triplet) methods with a 6-311G** basis set.

HA[52,53] is also listed in Table 1a for comparison with the computed ground state geometry. Figure 2 presents a comparison of the experimental normal Raman and FTIR spectra of HA, HA-^{13}C and HA-D_4 with the corresponding B3LYP/6-311G** calculated spectra based on the optimized structure shown in Figure 1. The comparison of the calculated IR and experimental FTIR spectra for HPDP is displayed in Figure 3. A Lorentzian function with 10 cm^{-1} bandwidth was used to produce vibrational bands for the calculated spectra. The calculated vibrational frequencies were scaled by a factor of 0.9718 and 0.9809 for HA and HPDP, respectively. The scaled factors minimize the root-mean-square difference between the calculated and experimental frequencies for bands with definitive or known identification.

Besides the structures (Figure 1) with the hydroxy O−H bond being cis to the carbonyl C═O bond, isomers with the O−H trans to the C═O were also calculated to be stable for both HA and HPDP. The computed total energy (including ZPE) of the trans conformation is very close to that of the cis isomer with the energy difference being less than 0.3 kcal/mol; the calculated IR and Raman spectra are also almost identical for the two isomers. They are hence indistinguishable, and both can contribute to the experimental spectra. Very similar results were found for the case of the triplets. We chose the cis conformation as representative in the discussion below for both the ground and triplet states.

Vibrational assignments to the experimental bands were made based on a direct comparison between the experimental and calculated spectra. A summary of the experimental and calculated vibrational frequencies and vibrational assignments for HA, HA-^{13}C, HA-D_4, HA-^{18}O, and HPDP are given in the Supporting Information. Vibrational coupling was found to be quite extensive for many vibrational modes, such as the ring C−C stretching

(48) Kihara, M.; Ikeuchi, I.; Kobayashi, Y.; Nagao, Y.; Hashizume, M.; Moritoki, H. *Drug Design Discov.* **1994**, *11*, 175−183.
(49) Banerjee, A.; Lee, K.: Falvey, D. E. *Tetrahedron* **1999**, *55*, 12699−12710.
(50) Ma, J. B.; Ji, Y. W.; Chen, H. C. *Chem. Reagent* **1991**, *13*, 191, 152.
(51) Gaussian 98, Revision A.7: Frisch, M. J.; Trucks, G. W.; Schlegel, H. B.; Scuseria, G. E.; Robb, M. A.; Cheeseman, J. R.; Zakrzewski, V. G.; Montgomery,J. A., Jr.; Stratmann, R. E.; Burant, J. C.; Dapprich, S.; Millam, J. M.; Daniels, A. D.; Kudin, K. N.; Strain, M. C.; Farkas, O.; Tomasi, J.; Barone, V.; Cossi, M.; Cammi, R.; Mennucci, B.; Pomelli, C.; Adamo, C.; Clifford, S.; Ochterski, J.; Petersson, G. A.; Ayala, P. Y.; Cui, Q.; Morokuma, K.; Malick, D. K.; Rabuck, A. D.; Raghavachari, K.; Foresman, J. B.; Cioslowski, J.; Ortiz, J. V.; Baboul, A. G.; Stefanov, B. B.; Liu, G.; Liashenko, A.; Piskorz, P.; Komaromi, I.; Gomperts, R.; Martin, R. L.; Fox, D. J.; Keith, T.; Al-Laham, M. A.; Peng, C. Y.; Nanayakkara, A.; Gonzalez, C.; Challacombe, M.; Gill, P. M. W.; Johnson, B.; Chen, W.; Wong, M. W.; Andres, J. L.; Gonzalez, C.; Head-Gordon, M.; Replogle, E. S.; Pople, J. A.; Gaussian, Inc., Pittsburgh, PA, 1998.
(52) Chenthamarai, S.; Jayaraman, D.; Meera, K.; Santhanaraghavan, P.; Subramanian, C.; Bocelli, G.; Ramasamy, P. *Cryst. Eng.* **2001**, *4*, 37−48.
(53) Vijayan, N.; Ramesh Babu, R.; Gunasekaran, M.; Gopalakrishnan, R.; Kumaresan, R.; Ramasamy, P.; Lan, C. W. *J. Cryst. Growth* **2003**, *249*, 309−315.

TABLE 1. Structural Parameters for the Ground and Triplet States of HA (a) and HPDP (b) Calculated from the DFT Calculations Using the B3LYP (Ground) and the UB3LYP (Triplet) Methods and a 6-311G Basis Set**

bond lengths (Å)				bond angles (deg)				dihedral angles (deg)			
	S_0	exptl (S_0)	T_1		S_0	exptl (S_0)	T_1		S_0	exptl (S_0)	T_1
C1−C2	1.398	1.371	1.405	C2−C1−C6	119.9	120.5	119.5	C6−C1−C2−C3	0.0		−0.5
C1−C6	1.400	1.378	1.405	C2−C1−O1	122.7	122.3	122.8	O1−C1−C2−C3	180.0		179.7
C1−O1	1.359	1.366	1.365	C1−C2−C3	119.8	118.2	120.7	C2−C1−C6−C5	0.0		−0.5
C2−C3	1.390	1.389	1.380	C2−C3−C4	121.0	122.7	120.9	C2−C1−O1−H1	0.0		1.3
C3−C4	1.400	1.387	1.429	C3−C4−C5	118.4	117.0	117.1	C6−C1−O1−H1	180.0		−178.5
C4−C5	1.404	1.390	1.435	C3−C4−C7	123.2	123.0	122.4	C1−C2−C3−C4	0.0		2.3
C5−C6	1.383	1.369	1.375	C4−C5−C6	121.3	121.1	121.3	C2−C3−C4−C5	0.0		−3.1
C4−C7	1.494	1.462	1.417	C1−C6−C5	119.7	120.5	120.4	C2−C3−C4−C7	180.0		179.2
C7−O2	1.217	1.216	1.317	C4−C7−O2	120.9	121.3	118.0	C3−C4−C5−C6	0.0		2.1
C7−C8	1.520	1.485	1.506	C4−C7−C8	118.8	120.0	126.1	C3−C4−C7−O2	180.0	173.1	161.9
				O2−C7−C8	120.3	118.7	115.2	C3−C4−C7−C8	0.0	6.9	−7.2
								C5−C4−C7−O2	0.0		−15.7
								C5−C4−C7−C8	180.0		175.1
								C4−C5−C6−C1	0.0		−0.4
								O2−C7−C8−H2	0.0		37.1

total energy[a] (hartree)	
S_0	T_1
−460.0995	−459.9894

bond lengths (Å)			bond angles (deg)			dihedral angles (deg)		
	S_0	T_1		S_0	T_1		S_0	T_1
P1−O2	1.472	1.472	P1−O3−C6	123.0	123.3	O19−C16−C15−C14	179.9	179.3
P1−O3	1.595	1.592	P1−O4−C8	122.7	120.2	C15−C14−C13−C11	−179.9	−179.1
P1−O4	1.593	1.603	P1−O5−C10	120.3	121.6	C18−C13−C11−C10	2.6	−11.2
P1−O5	1.628	1.623	O2−P1−O3	113.6	114.5	C14−C13−C11−C10		
O3−C6	1.450	1.451	O2−P1−O4	119.3	117.5	C13−C11−C10−O5	175.2	85.5
O4−C8	1.461	1.455	O2−P1−O5	113.4	114.0	C11−C10−O5−P1	92.2	121.3
C6−C7	1.514	1.514	O3−C6−C7	107.7	107.6	C10−O5−P1−O3	114.8	129.3
C8−C9	1.515	1.514	O4−C8−C9	109.8	107.7	C10−O5−P1−O4	−139.8	−125.0
O5−C10	1.422	1.461	O5−C10−C11	111.7	111.4	O5−P1−O3−C6	55.0	55.3
C10−C11	1.533	1.497	C10−C11−O12	120.4	116.7	O5−P1−O4−C8	73.4	76.4
C11−O12	1.215	1.314	C10−C11−C13	117.7	125.1	P1−O3−C6−C7	−176.2	−179.2
C11−C13	1.487	1.427	C11−C13−C14	118.3	120.2	P1−O4−C8−C9	−112.5	−172.4
C13−C14	1.405	1.431	C13−C14−C15	121.2	121.2	C18−C13−C11−O12	−177.6	156.9
C14−C15	1.382	1.376	C14−C15−C16	119.7	120.2	C14−C13−C11−O12	2.0	−20.7
C15−C16	1.401	1.404	C15−C16−C17	120.0	119.7	O5−C10−C11−O12	−4.6	−82.6
C16−C17	1.398	1.407	C16−C17−C18	119.8	120.5	C10−C5−P1−O2	−9.3	3.7
C17−C18	1.389	1.379	C18−C13−C14	118.4	117.5	O2−P1−O4−C8	−53.4	−50.2
C18−C13	1.401	1.426	C18−C13−C11	123.3	122.3	O2−P1−O3−C6	179.0	−179.4
C16−O19	1.358	1.360	C15−C16−O19	117.3	117.6			
O19−H20	0.963	0.963	C16−O19−H20	109.7	109.6			

total energy[a] (hartree)	
S_0	T_1
−1260.2830	−1260.1762

[a] Including zero-point energy.

motions that couple with the ring-substituted stretching and the ring C−H bending vibrations that couple with the hydroxy O−H bending vibrations. The descriptions of the assignments are based on the atomic displacements of the calculated normal mode and the depictions listed in the tables of the Supporting Information (Tables 1S−4S) include only vibrations with predominant contributions to the corresponding vibrational modes. Where applicable, the Wilson notation[54] is used to label the ring C−H and C−C vibrations analogous to benzene motions.

It can be seen from Figure 1a and Table 1a that the optimized structure of the ground state HA has C_s symmetry with both the hydroxyl and carbonyl groups within the ring plane. Computations using C_1 symmetry lead to an optimized structure almost identical to those resulting from the C_s calculation. We therefore take the C_s-optimized structure for our discussion on the ground-state conformation. Comparison between the X-ray data[52] and our calculated results shows that the differences in the bond lengths are within 0.035 Å and those for the bond angle are less than 1.7°, indicating reasonable agreement between the DFT computation and the X-ray measurements. However, we note that, unlike the calculated planar structure, the X-ray result shows that the carboxylic carbon atom (C(7)) is displaced by 0.0376 Å from the ring plane and the C(=O)CH_3 group is reported to form a 6.9° dihedral angle with respect to the aromatic ring for crystallized HA. This might be mainly due to the intermolecular hydrogen bonding interactions and a packing effect that have been found to be very extensive in crystalline HA.[52,53] Our planar structure is in agreement with recent theoretical results for several analogous aromatic carbonyl compounds[55,56] and can be attributed to the extended conjugation interaction between the ring π system with the C=O π orbital. One indication for this

(54) Varsanyi, G. *Assignments for vibrational spectra of seven hundred benzene derivatives*; Lang, L., Ed.; Adam Hilger: London, 1974; Vol. I.

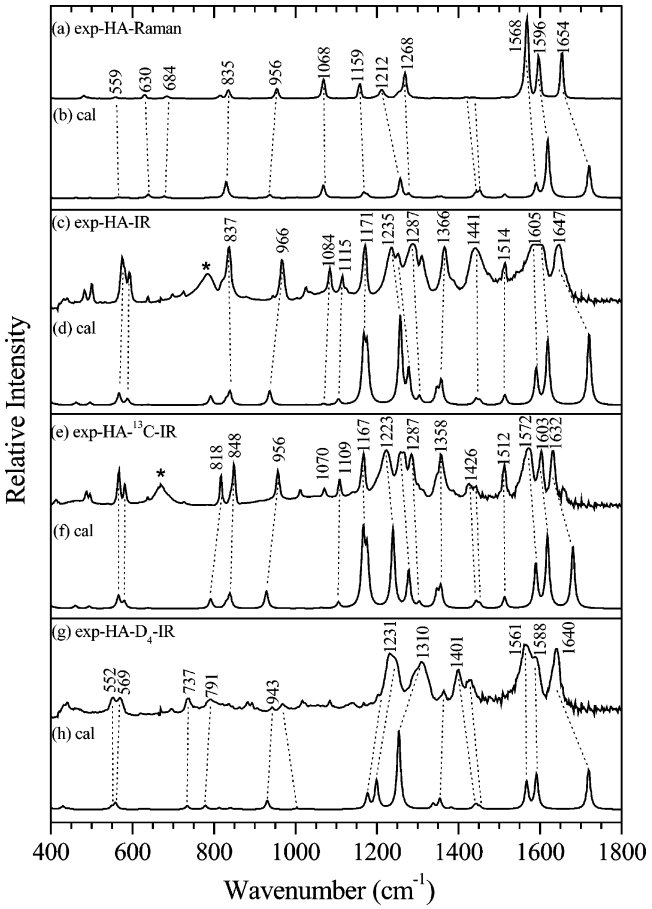

FIGURE 2. Comparison of the experimental and DFT calculated Raman and IR spectra for the ground state of HA, HA-^{13}C and HA-D_4. The asterisk (*) marks an ambient or stray light artifact band. See the text for more details.

is that the bond length of C−C bond connecting the ring and carbonyl subgroups (C(4)−C(7)) is calculated to be 1.49 Å, and this is shorter than the ∼1.52 Å normal C−C single bond length.

To our knowledge, there has been no X-ray diffraction data published in the literature for HPDP that can be used for comparison to the calculated geometry. It can be seen from Figure 1b and Table 1b that, except for the slight twisting (by ∼2°) of the ring connected −C(═O)CH_2− subgroup with respect to the ring plane, the calculated geometric parameters related to the *p*-hydroxyphenacyl subgroup are very similar to those in HA. We note also that the *p*-hydroxyphenacyl conformation in HPDP is almost identical to that in *p*-hydroxyphenacyl acetate (HPA).[16] This may imply that the structure of the *p*-hydroxyphenacyl cage structure is little affected by the existence or the type of leaving group. Similar to the calculated structure of HPA, the O(5) atom joining the phosphate and the *p*-hydroxyphenacyl cage in HPDP is found to be nearly in the same plane defined by the ring with the nearby H32 and H31 atoms on opposite sides of the plane.

Inspection of Figures 2 and 3 shows that the experimentally recorded Raman and IR spectra agree reasonably well with the B3LYP/6-311G** computed spectra for both HA and HPDP, respectively. This confirms again that the optimized structures from the B3LYP/6-311G** computation are reasonable, and this makes assignments of the vibrational bands relatively straightforward. By comparing the results for HPDP with HA, one can find that the *p*-hydroxyphenacyl group related local vibrational modes, such as the carbonyl C═O stretching, the ring C−C stretching dominated by the Wilson 8a, 8b, and 19a, the ring C−H in-plane bending (the Wilson 9a, 18b) and out-of-plane bending, have the frequencies that appear at similar positions: 1660, 1609, 1579, 1516, 1171, 1117, and 774 cm^{-1} for HPDP and 1647, 1605, 1587, 1514, 1171, 1115, and 783 cm^{-1} for HA. This is consistent with the geometry results mentioned above. For a discussion of the triplet structure and the deprotection mechanism of the phenacyl caged compounds, it is necessary to mention here the mode dominated by the C10−O5 stretching vibration for HPDP (the motion leading to direct cleavage of the phosphate leaving group from the phenacyl cage structure). The mode with the largest contribution from the C10−O5 stretching is at 1105 cm^{-1} but it can be seen from Table 2S (Supporting Information) that this mode is mixed in character and couples with the ring C−H in-plane bending and the phosphate methyl group rocking vibrations.

It is obvious from Figures 2 and 1S (Supporting Information) that the ^{13}C and D_4 isotopic substitutions of HA lead to substantial changes of the vibrational spectrum in terms of band frequencies and spectral profiles. It is also clear that these changes are reproduced reasonably well by the DFT calculations. Comparison of the experimental and calculated IR spectra in Figure 2c,d with those in Figure 2e,f shows that, on going from the normal HA to HA-^{13}C, there are generally small changes in the relative intensities for the corresponding bands, but several bands display obvious frequency downshifts upon the ^{13}C substitution. These bands are from modes with vibration related to the carbonyl carbon atom (C7 in Figure 1a). This is confirmed by the DFT calculations. For example, the carbonyl C═O stretching vibration shifts down by ∼15 cm^{-1} from 1647 cm^{-1} for HA to 1632 cm^{-1} for HA-^{13}C; the mode dominated by the ring-carbonyl stretching (C4−C7 stretching at 1235 cm^{-1} for HA) and that contributed by C4−C7 out-of-plane (1024 cm^{-1} for HA) and in-plane (966 cm^{-1} for HA) bending motion shift down by ∼12, 12, and 10 cm^{-1}, respectively, upon the ^{13}C substitution (Table 1Sa, Supporting Information). The computed frequency downshifts are 39, 18, 11, and 8 cm^{-1}, respectively, for these modes, consistent with the experimental observation.

Comparison of the IR spectra and the results of vibrational analysis between the normal (Table 1Sa (Supporting Information), Figure 2c,d) and D_4 deuterated HA (Table 1Sb (Supporting Information), Figure 2g,h) shows that the frequency shifts are not restricted to the ring CH mode since there are also complex changes in vibrational coupling between this and other modes within the ring deuterated molecule that affect both frequencies and intensities.[57−60] To help interpret the excited state

(55) Wang, Y.-W.; He, H.-Y.; Fan, W.-H. *TheoChem* **2003**, *634*, 281−287.

(56) Fang, W. H.; Phillips, D. L. *ChemPhysChem* **2002**, *3*, 889−892

(57) Kwok, W. M.; Ma, C.; Matousek, P.; Parker, A. W.; Phillips, D.; Toner, W. T.; Towrie, M.; Umapathy, S. *J. Phys. Chem. A* **2001**, *105*, 984−990.

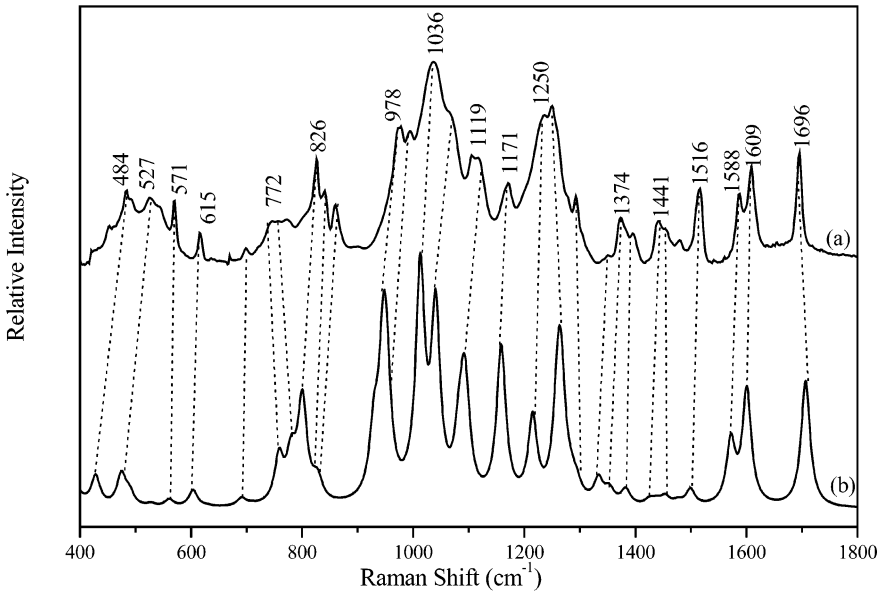

FIGURE 3. Comparison of the experimental (a) and DFT calculated (b) IR spectra for the ground state of HPDP. See the text for more details.

TABLE 2. Spin Density Distribution for the Triplet States of HA and HPDP Obtained from the DFT UB3LYP/6-311G Calculations**

HA		HPDP	
ρC1	0.257	ρP1	0.003
ρC2	−0.085	ρO2	0.002
ρC3	0.225	ρC3	0.003
ρC4	0.014	ρO4	0.001
ρC5	0.221	ρO5	0.035
ρC6	−0.114	ρC6	0.000
ρC7	0.452	ρC7	0.000
ρC8	0.014	ρC8	0.000
ρO1	0.057	ρC9	0.000
ρO2	0.922	ρC10	0.043
		ρC11	0.462
		ρO12	0.884
		ρC13	0.040
		ρC14	0.195
		ρC15	−0.098
		ρC16	0.240
		ρC17	−0.062
		ρC18	0.192
		ρO19	0.064

spectra, it is worthwhile to mention several points relating to the typical band shifts and variations of vibrational features on going from the normal to HA-D_4. The ring C−H stretching modes shift down by ∼800 cm^{-1} from ∼3100 cm^{-1} in normal HA to ∼2300 cm^{-1} in HA-D_4 (Table 1S, Supporting Information). Consistent with the calculation, the four downshifted C−H stretching bands have been observed clearly in the experimental FT-IR spectra verifying the identification and purity of the synthesized HA-D_4 sample. The comparison between the experimental and calculated spectra for HA-D_4 in this spectral region is provided in the Supporting Information. Bands dominated by the ring CC stretching vibrations were found to shift down by ∼15−30 cm^{-1}, such as the Wilson 8a and 8b modes that shift from 1605 and 1587 cm^{-1} for normal HA to 1588 and 1562 cm^{-1}, respectively, for HA-D_4. The ring C−H bending dominated mode shift down by ∼300−400 cm^{-1} upon ring deuteration. Some examples are the frequencies of the ring C−H in-plane bending modes where the Wilson 3, 9a, and 18b vibrations shift from 1287, 1171, and 1115 cm^{-1} in normal HA to 966, 818, and 791 cm^{-1}, respectively, in HA-D_4. Modes showing substantial changes in vibrational coupling components upon the ring deuteration are strongly mixed modes, for example, those associated with the ring-substituent stretching vibrations, i.e., C4−C7 and C1−O1, and the ring C−C stretching described by the Wilson 19a and 19b. These modes couple extensively with the ring C−H bending vibrations in normal HA. However, the calculations show that the contributions of the C−H bending motions are reduced or vanished in the corresponding modes for HA-D_4. This can lead to frequency downshifts as well as upshifts on going from the normal HA to HA-D_4. Examples include modes dominated by the Wilson 19a and 19b vibrations that show frequency downshifts, whereas modes dominated by the ring-substitution stretching motion exhibit upshifts from normal HA to HA-D_4.

B. Time-Resolved Resonance Raman Spectra. Figures 4 and 5 display representative ps- and ns-TR[3] spectra of HA and HPDP, respectively, in acetonitrile acquired with pump and probe time delays varying from 0 to 200 ns for HA and 300 ns for HPDP. Only the bands observed for the 500−2000 cm^{-1} region are shown in Figures 4 and 5 since there were no obvious features recognized below 400 cm^{-1} or in the 2000−3500 cm^{-1} region. For both HA and HPDP, comparison of the spectra in Figures 4b and 5b with those in Figures 4a and 5a, respectively, reveals that the spectral features observed on the nanosecond time scale are the same as those that appear in corresponding later time picosecond

(58) Kwok, W. M.; Ma, C.; Parker, A. W.; Phillips, D.; Towrie, M.; Matousek, P.; Phillips, D. L. *J. Chem. Phys.* **2000**, *113*, 7471−7478.
(59) Ma. C.; Kwok, W. M.; Matousek, P.; Parker, A. W.; Phillips, D.; Toner, W. T.; Towrie, M. *J. Photochem. Photobiol. A* **2001**, *142*, 177−185.
(60) Kwok, W. M.; Gould, I.; Ma, C.; Puranik, M.; Umapathy, S.; Matousek, P.; Parker, A. W.; Phillips, D.; Toner, W. T.; Towrie, M. *Phys. Chem. Chem. Phys.* **2001**, *3*, 2424−2432.

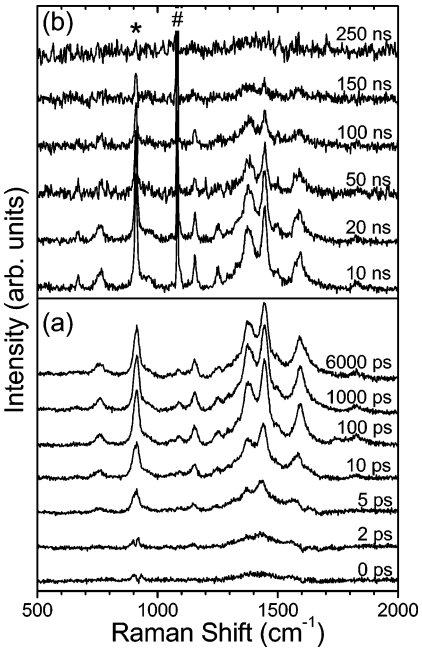

FIGURE 4. Picosecond (a) and nanosecond (b) time-resolved resonance Raman spectra of HA in acetonitrile obtained with a 266 nm pump excitation wavelength and 400 nm (picosecond spectra) and 416 nm (nanosecond spectra) probe wavelengths at various time delays that are indicated on the spectra. The nanosecond spectra were obtained under nitrogen purge conditions. The asterisks (∗) mark solvent subtraction artifacts. The # band is due to a stray laser line.

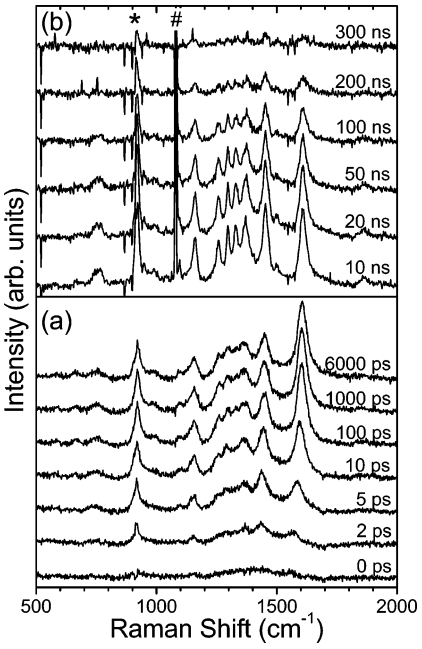

FIGURE 5. Picosecond (a) and nanosecond (b) time-resolved resonance Raman spectra of HPDP in acetonitrile obtained with a 266 nm pump wavelength and 400 nm (picosecond spectra) and 416 nm (nanosecond spectra) probe wavelengths at various time delays that are indicated on the spectra. The nanosecond spectra were recorded under nitrogen purge conditions. The asterisks (∗) mark solvent subtraction artifacts. The # band is due to stray laser line.

spectra (20 ps and afterward). This indicates that the same species are detected in both the cases. The slight differences in the relative intensity between the picosecond and nanosecond spectra can be attributed to the different probe wavelengths used for the respective TR^3 measurements (400 nm in ps-TR^3 vs 416 nm in ns-TR^3). In addition, it can be seen that the bandwidths for features in the picosecond spectra are generally broader than those in the nanosecond ones. Take the 910 cm^{-1} band in HA for example. Fits to the experimental band with a Lorentzian band shape results in a FWMH of ∼13 and 26 cm^{-1} for a nanosecond and late picosecond spectrum, respectively. The broadness of the ps-TR^3 bands is therefore obviously due to the convolution of the intrinsic Raman bandwidth with the line width (∼15 cm^{-1}) of the picosecond laser pulse. The better spectral resolution of the nanosecond TR^3 spectra allows features that are overlapped in the picosecond spectra to be resolved clearly in the nanosecond spectra. For example, the four features of HDPD, 1257, 1297, 1330, and 1371 cm^{-1} are resolved clearly in the nanosecond spectra (Figure 5 b) but appear as an overall broad shoulder in the picosecond spectra.

From Figures 4 and 5, it can be seen for both HA and HPDP that the initial picosecond spectra (the 0−2 ps spectrum) are almost featureless but develop rapidly at very early times and decay in intensity on the nanosecond time scale. By fitting the Raman features with Lorentzain band shapes, Figures 6b and 7b display the time-dependence of the ∼1600 cm^{-1} band areas in 0−100 ps time scale for HA and HPDP, respectively. Decay of this band on the nanosecond regime observed under nitrogen purge conditions are shown in Figures 6a and 7a, respectively, for the two compounds. As displayed together with the experimental data points, the kinetics shown in Figures 4 and 5 can be fit well by one exponential growth or decay function for both the picosecond and nanosecond data for the two compounds. A time constant of 5.3 and 6.7 ps, respectively, was found for the early time growth and 86 and 150 ns, respectively, for the nanosecond decay of HA and HPDP.

During the experiments, it was found that the nanosecond decay rates of both of the compounds increase under open-air conditions, and the lifetimes were reduced to less than 10 ns when the sample system was bubbled with oxygen. These observations suggest that the transient species detected here is triplet in nature, and this is consistent with the previous results of Wan and co-workers[14] and Givens and co-workers.[9,11,12] These two groups report that the triplet state is the sole intermediate formed by excitation of the *p*-hydroxyphenacyl caged compounds in acetonitrile solvent. The published triplet-state transient absorption data show that spectra of both of the two compounds have a strong absorption around the 400 nm probe wavelength used here for the TR^3 measurements, implying that the vibrational bands of the triplet state will be resonance enhanced in the present experiments. This leads to further support to the triplet-state assignment of the ps- and ns-TR^3 spectra. However, we note that the lifetime of HA obtained here (86 ns) is noticeably shorter than the 700 ns lifetime reported by Wan and co-workers[14] and could be due to trace amounts of oxygen still being present in our sample. To our knowledge, there is no triplet-state lifetime information available for HPDP in the literature. We attribute our shorter lifetime as being due to the degas-

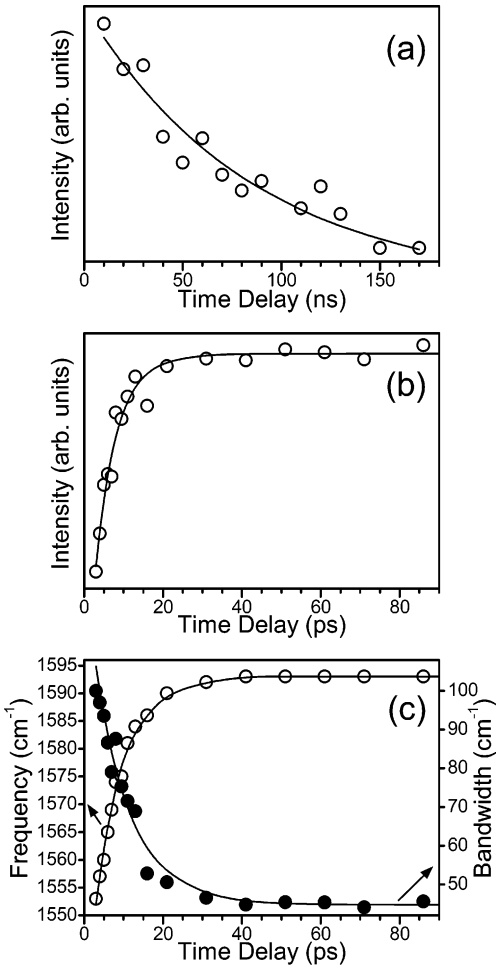

FIGURE 6. (a) Time-dependence of the HA triplet 1594 cm^{-1} band areas obtained in the nanosecond time-resolved Raman measurements. (b) Time-dependence of the 1594 cm^{-1} band areas obtained in the picosecond time-resolved Raman measurement under nitrogen purge conditions. (c) Time dependence of the 1594 cm^{-1} bandwidth (filled circle) and frequency (open circle) obtained in the picosecond time-resolved Raman measurement. Solid lines are results of fits to the experimental data (see text).

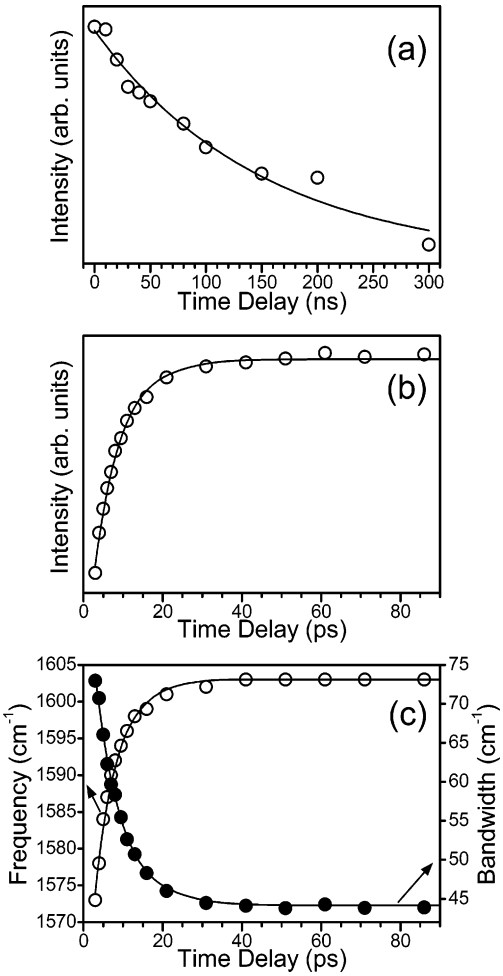

FIGURE 7. (a) Time-dependence of the HPDP triplet 1612 cm^{-1} band areas obtained in the nanosecond time-resolved Raman measurement under nitrogen purge conditions. (b) Time-dependence of the 1612 cm^{-1} band areas obtained in the picosecond time-resolved Raman measurement. (c) Time dependence of the 1612 cm^{-1} bandwidth (filled circle) and frequency (open circle) obtained in the picosecond time-resolved Raman measurement. Solid lines are results of fits to the experimental data (see text).

sing method used in our experiment being not efficient enough to reduce the concentration of residual oxygen to a small enough value to get a very accurate lifetime of the triplet state in the absence of oxygen. This is quite possible since the sample arrangement used for the experiment is an open-air recirculated system.

To validate further the triplet state assignment, we have recently carried out femtosecond Kerr-gated time-resolved fluorescence (KTRF) measurements on the two compounds. These experiments were done with 266 nm excitation in acetonitrile. Temporal evolution of the fluorescence intensity and the fluorescence spectral profile were found to be almost identical for the two compounds and a ~2 ps time constant was found for the decay of the fluorescence intensities. This implies that ISC conversion from the singlet to triplet state occurs with a rate of $\sim 5 \times 10^{11}$ s^{-1} for both the compounds.[61] The ISC rate is close to reported value of 2.7×10^{11} s^{-1} and $3.8 \pm 0.2 \times 10^{11}$ s^{-1} for HA and HPDP, respectively.[9] These results are also consistent with the general view that aryl carbonyl compounds have high ISC yields and rapid ISC rates.[17,62−64] More importantly, we note that the ISC rate correlates with the rapid growth of the TR^3 spectra in the early picosecond time range. This provides additional verification that the intermediates we observed are indeed from the triplet state of HA and HPDP.

By carefully checking the early picosecond spectra (Figures 4a and 5a), we found that, besides the intensity changes, the frequency and bandwidth of the Raman features also show temporal changes with a time constant similar to the growth of the band intensity. The frequency shifts up and bandwidth becomes narrower within the first 20 ps. Taking the ~1600 cm^{-1} band as an example,

(61) Ma, C.; Kwok, W. M.; Chan, W. S.; Zuo, P.; Phillips, D. L. Unpublished work.

(62) Rentzepis, P. M. *Science* **1970**, *169*, 239−247.
(63) Damschen, D. E.; Merritt, C. D.; Perry, D. L.; Scott, G. W.; Talley, L. D. *J. Phys. Chem.* **1978**, *82*, 2268−2272.
(64) Baronavski, A. P.; Owrutsky, J. C. *Chem. Phys. Lett.* **2001**, *333*, 36−40.

the early time (0−100 ps) time dependencies of frequency and bandwidth changes are displayed in Figures 6c and 7c for HA and HPDP, respectively. The changes observed can be fit by one exponential with a time constant of ∼5−8 ps for both of the compounds. We attribute this observation to the triplet state relaxation of excess energy from the rapid ISC conversion and formation of an unrelaxed energetic triplet state. It has been well-recognized and demonstrated by ultrafast TR^3 spectroscopy that relaxation of excess energy produces band changes of such as those observed here in the TR^3 spectra on a very similar time scale.[65−69] Consistent with this, the generation of a vibronically excited triplet state due to the rapid ISC from an excited singlet state has been suggested for aromatic carbonyl compounds in previous studies.[62,70]

In the present TR^3 measurements, the 267 nm pump wavelength lies in the lowest strong absorption band of HA and HPDP (UV absorption spectra are similar for the two compounds in acetonitrile). The absorption originates from the allowed $S_0 \rightarrow S_3$ ($^1\pi\pi^*$) transition of the HA chromphore. A study of the singlet → triplet transition by the phosphorescence excitation method found that the $S_0 \rightarrow T_1$ absorption appears at 395 nm for HA.[33] The high triplet state yield and extremely short lifetime of the singlet excited states[31,62] indicate that the ISC process is the predominant deactivation pathway for most photoexcited aromatic carbonyls including the *p*-hydroxyphenacyl caged compounds. We can therefore estimate that the 267 nm excitation could introduce more than 12 000 cm^{-1} of excess energy, the availability of which can be responsible for the early time dynamics of the frequencies and bandwidth evolution observed here in the ps-TR^3 spectra.

It is interesting to point out that the ∼5−8 ps time constant for the changes of frequency and bandwidth match well with the 5.3 (HA) and 6.7 ps (HPDP) time constant of the intensity growth. Although the early time development of the band intensity has been explained vide supra as due to the formation of the triplet state, this match may imply that, besides the ISC conversion, the excess energy relaxation process is also responsible, at least partially, for the early stage dynamics of the band intensity for both the compounds. This provides an interpretation for the small but noticeable difference between the fluorescence decay time, i.e., ISC time constant (∼2 ps), and the relatively longer 5.3 or 6.7 ps growth of the triplet-state spectra.

According to the preceding descriptions and analysis, it is clear that the ISC rate and dynamics of the excess energy relaxation processes are quite similar for both the parent HA molecule and the caged compound HPDP. We note that such a similarity applies also to *p*-hydroxyphenacyl acetate (HPA) with the acetate as leaving group.[16] This may imply that the ISC and excess energy relaxation processes are independent of the existence of and the type of leaving groups. This means that these processes and the photoexcitation absorption as well are localized on the *p*-hydroxyphenacyl chromophore and are little affected by the leaving group. Further discussion on this point will be presented later in the paper.

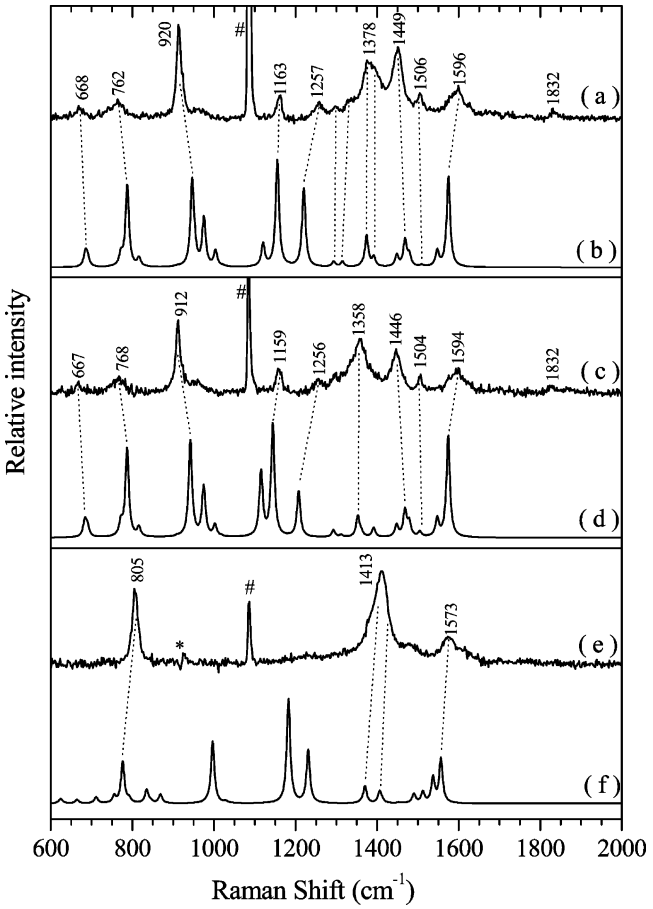

FIGURE 8. Comparison of the experimental resonance Raman spectra of the triplet state of HA (a), HA-^{13}C (c) and HA-D_4 (e) with the corresponding DFT calculated triplet state Raman spectrum (b), (d), and (f). The asterisks (∗) mark solvent subtraction artifacts. The # marks the band due to scattering from the laser line.

C. Assignment of the Triplet State Spectrum of HA. The optimized geometry and relevant structural parameters of the triplet HA, obtained from the open-shell DFT calculations, are given in Figure 1a and Table 1a, respectively, for comparison with the corresponding ground-state results. The other details of the geometry parameters and the total energy obtained from DFT computations are listed in Supporting Information. In Table 1a, we have also listed the calculated total energies including the zero point energies, for both the triplet and ground states, from which a 69.0 kcal/mol triplet-state energy can be calculated. This triplet-state energy is in good agreement with the observed 70.5 kcal/mol experimental value and is also comparable to the 69.6 kcal/mol calculated result reported by Wirz and co-workers.[9]

Figure 8 displays a comparison between the experimental and calculated triplet state spectra for normal HA, HA-^{13}C, and HA-D_4. No scale factor was used for the

(65) Ma. C.; Kwok, W. M.; Matousek, P.; Parker, A. W.; Phillips, D.; Toner, W. T.; Towrie, M. *J. Raman Spectrosc.* **2001**, *32*, 115−123.
(66) Matousek, P.; Parker, A. W.; Towire, M.; Toner, W. T. *J. Chem. Phys.* **1997**, *107*, 9807−9817.
(67) Iwata, K.; Hamaguchi, H. J. *J. Phys. Chem. A* **1997**, *101*, 632−637.
(68) Hester, P. E.; Matousek, P.; Moore, J. N.; Parker, A. W.; Toner, W. T.; Towire, M. *Chem. Phys. Lett.* **1993**, *208*, 471−478.
(69) Weaver, W. L.; Huston, L. A.; Iwata, K. Gustafson, T. L. *J. Phys. Chem.* **1992**, *96*, 8956−8961.
(70) Berger, M.; Steel, C. *J. Am. Chem. Soc.* **1975**, *97*, 4817−4821.

calculated spectra of HA and HA-^{13}C, but a 1.014 factor was used to scale the calculated spectrum of HA-D_4, so as to obtain a better match to the experimental spectrum. It can be seen that the calculations reproduce reasonably well the experimental spectra, especially in the cases of HA and HA-^{13}C. Some differences in the relative intensities among the various features between the experimental and calculated spectra are within expectations since the former is obtained with resonance enhancement while the latter corresponds to a normal Raman spectrum for the triplet state. Preliminary assignments have been made through a comprehensive consideration of the isotopic shifts as well as the correlation between the experimental (Figure 8a,c,e) and calculated (Figure 8b,d,f) spectra. It can be seen that the DFT computation reproduces the experimental spectra reasonably well, and most of the spectral changes caused by the isotopic substitutions are also reproduced by the calculations. The observed triplet state band frequencies together with the corresponding computed values and their preliminary assignments are provided in the Supporting Information.

Most features observed in the triplet state spectra are mainly from vibrations of the ring C−C stretching, the ring C−H bending, and the ring-substitution stretching motions. In the normal spectrum (Figure 8a,b), the 1594 (and its left-hand shoulder band), 1506, 762, and 637 cm^{-1} features are mainly due to various ring C−C stretching vibrations. The 1325, 1257, 1158, 1095, and 920 cm^{-1} bands are predominately from various ring C−H in-plane or out-of-plane bending motions coupled differently with the ring C−C or other vibrations related to the substituent group. Among these bands, the 1257 cm^{-1} band has a modest contribution from the carbonyl C−O stretching motion. According to the DFT computation, the 1257 cm^{-1} band is the only one with a significant C−O stretching contribution, or in an other words, there was no localized carbonyl C−O stretching mode found for the triplet state of HA. The strong feature at 1378 cm^{-1} and the weak feature at 1296 cm^{-1} are found to be mixed modes with contributions mainly from the ring-$C(O)CH_3$ and ring-OH stretching, respectively, and coupling with the ring C−H in-plane bending vibrations. The 1449 cm^{-1} feature can be attributed to the CH_3 group deformation vibration. The broadness of this feature may imply that it could include an additional nearby feature that is from a ring C−C stretching, according to the calculation results.

The Raman band assignments described above agree well with the isotopic shifts observed and calculated in the HA-^{13}C and HA-D_4 spectra. Such as the assignment of the normal 1378 cm^{-1} band to the ring-$C(O)CH_3$ stretching is confirmed by the ∼20 cm^{-1} downshift of the band frequency to the 1358 cm^{-1} in the experimental HA-^{13}C spectrum (Figure 8a,c)) and the ∼20 cm^{-1} downshift in the corresponding calculated spectrum. The result that the mode is insensitive to the carbonyl ^{18}O (Table 2Sa, Supporting Information) implies it has little contribution from the carbonyl CO stretching motion. The assignment of the 1573 cm^{-1} HA-D_4 band to the ring C−C stretching (Wilson 8a) is straightforward. The band shifts downward by ∼24 cm^{-1} from the corresponding normal band. The amount of the shift is very close to that observed in the corresponding ground-state band on going from the normal to ring deuterium HA. According to the calculation, the substantial spectral differences between HA-D_4 (Figure 8e) and those of normal and ^{13}C substituted HA are due to changes in the vibrational coupling pattern and redistribution of the potential energy related to the relevant modes induced by the ring deuteration.[57−61,71,72] It is quite certain that the rather weak feature at ∼1832 cm^{-1} in the experimental normal HA and HA-^{13}C spectra is from the first overtone of the 910 cm^{-1} band. The lack of this band in the HA-D_4 spectrum is due to the absence of this fundamental in that spectrum.

Identification of the triplet-state carbonyl CO stretching mode is important since it has been suggested by previous vibrational studies that the frequency of this mode can be taken as a direct indication for the nature of the triplet state in term of its $n\pi^*$ or $\pi\pi^*$ electronic configuration.[34,38,73] The isotopic shift data is diagnostic for identifying such a mode. In the ground state, the CO stretching mode is at 1647 cm^{-1} (IR) for normal HA, and it shifts downfield by 15 and 24 cm^{-1}, respectively, upon carbonyl ^{13}C and ^{18}O substitution.[38] The mode is local in character, and its frequency is insensitive to ring deuteration and appears at 1640 cm^{-1} in the HA-D_4 spectrum (Figure 2 and Table 1S (Supporting Information)). However, the experimental isotopic data for the HA triplet state shown in Figure 8 and Table 3S (Supporting Information) shows that no band displays a similar isotopic shift behavior in the triplet state. This observation combined with the theoretical data for the HA, HA-^{13}C, and HA-D_4 molecules indicates that there is no localized CO stretching mode for the HA triplet state. It is possible, however, that the CO stretching motion could couple slightly with other vibrations of similar frequency. As illustrated above, the normal band at 1257 cm^{-1} is the most probable candidate. We cannot completely rule out the possibility that the distinct CO mode is not resonantly enhanced by the probe wavelengths used in the present TR^3 measurement. However, the reasonably good agreement between the experimental and calculated results leads us to believe that this is not the case. Further discussion on this point is given below.

D. Assignment of the Triplet-State Spectrum of HDPD. The optimized geometry and relevant structural parameters of the HPDP triplet state are given in Figure 1b and Table 1b for comparison with the corresponding ground state data. The full geometry parameters and computed total energy from the DFT calculations are listed in the Supporting Information. The computed total energies, including the ZPE, have also been listed in Table 1b for both the triplet and ground states, from which a 67.0 kcal/mol triplet-state energy was estimated. This triplet-state energy is close to the experimental value of 70.6 kcal/mol derived from the phosphorescence measurements of HPDP.[8,9] Figure 9 displays a comparison between the experimental and unscaled calculated triplet spectra. It can be seen that the calculations reproduce the experimental spectrum reasonably well. This allows straightforward assignment of the experi-

(71) Okamoto, H.; Inishi, H.; Nakamura, Y.; Kohtani, S.; Nakagaki, R. *Chem. Phys.* **2000**, *260*, 193-214.
(72) Okamoto, H.; Inishi, H.; Nakamura, Y.; Kohtani, S.; Nakagaki, R. *J. Phys. Chem. A* **2001**, *105*, 4182−4188.
(73) George, M. W.; Kato, C.; Hamaguchi, H. *Chem. Lett.* **1993**, *5*, 873−876.

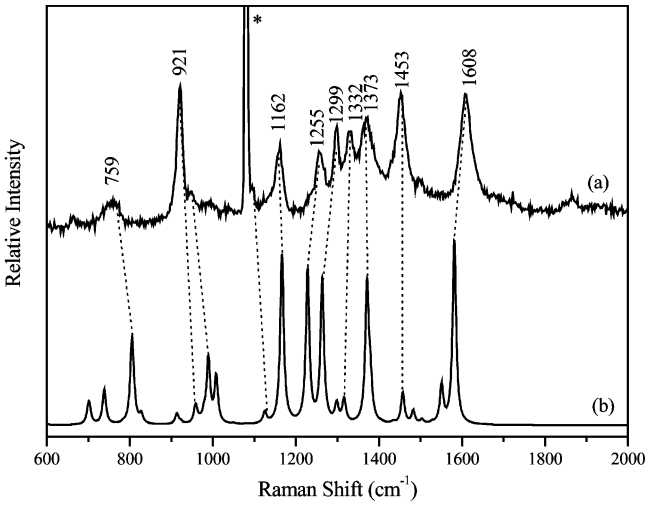

FIGURE 9. Comparison of the experimental resonance Raman spectra of the triplet state of HPDP (a) with the DFT calculated triplet state Raman spectrum (b).

mental bands by associating the corresponding features in the two spectra. The details of the triplet state frequencies and vibrational assignments are given in the Supporting Information.

By comparing the triplet state vibrational assignments for HDPD (Table 4S, Supporting Information) with that for HA (Table 3S, Supporting Information), it can be seen that the resonance enhanced bands observed experimentally for both compounds are mostly from similar vibrational modes and appear at comparable frequencies. For example, the ring C−C stretching related modes are found to be at 1594, 1506, and 762 cm^{-1} for HA (above) and at 1612, 1504 (calculated), and 768 cm^{-1}, respectively, for HPDP; the ring C−H bending dominated modes at 1325, 1296, 1257, 1158, 1095, and 920 cm^{-1} for HA that appear at 1330, 1297, 1257, 1162, 109, and 921 cm^{-1}, respectively, for HPDP. In addition, like the case of HA, there is also a weak feature at ∼1850 cm^{-1} in the HPDP spectrum, which was attributed analogously to the first overtone of the 921 cm^{-1} mode. This similarity indicates that (i) the *p*-hydroxyphenacyl chromophore is responsible for the triplet state resonance enhancement promoted by the probe wavelengths (400 or 416 nm) in HPDP and (ii) the existence of the phosphate leaving group has little influence on the geometry of the *p*-hydroxyphenacyl moiety in the triplet excited state.

However, although there are significant similarities, we also note some differences between the triplet-state spectra of HA and HPDP. Comparison of the HPDP spectrum in Figure 9a with the HA spectrum in Figure 8a shows that the relative intensity distribution of the bands in HPDP is not the same as that in HA. An example of this is the intensity ratio between the ∼1600 to ∼1450 cm^{-1} features is higher in HPDP than in HA. Also, taking the ∼1370 cm^{-1} feature as a reference, the relative intensities of the features at ∼1257, 1297, and 1370 cm^{-1} are substantially larger in HPDP than in HA. These results mean that, although only modestly, the leaving group does induce some modest perturbation, probably in regard to slight modification of the electronic configuration, on the triplet state properties and structure.

Moreover, there appears to be an additional feature at ∼913 cm^{-1} in the experimental spectrum of HPDP, compared with the spectrum of HA. A feature at 913 cm^{-1} has been calculated for the HPDP triplet state (Figure 9c and Table 4S, Supporting Information). The existence of a nearby strong feature at ∼920 cm^{-1} and involvement of a solvent band at a similar position causes some uncertainty on the identification of this feature. It was found to be mainly from a C−O stretching vibration that could lead to cleavage of the leaving group from the *p*-hydroxyphenacyl "cage". The counterpart of this stretching vibration in the ground state is at 1105 cm^{-1} (above). If this triplet state vibrational band assignment is correct, then this band shifts downfield by about 190 cm^{-1} in going from the ground to triplet state, indicating that the C10−O5 bond becomes obviously weakened in the triplet state compared to the ground state. This is consistent with the triplet state structural data presented below.

E. Structure and Nature of the Triplet States of HA and HDPD. It can be seen from Figure 1 and Table 1 that, for both HA and HPDP, the molecular structure changes significantly in going from the ground state to the triplet state and that the extent and trend of the changes are quite similar for the two molecules. For HA, the triplet state is found to have C_1 symmetry due to the twisting of the $-C(O)CH_3$ group and rotation of the $-CH_3$ group around the −C(O)−C bond. This leads to the breaking of the ground state C_s symmetry. Thus, the plane constituted by the carbonyl group and the $-CH_3$ group carbon atom is found to twist out of the ring plane by ∼16° in the triplet state, compared with the ground state, and the $-CH_3$ group rotates around the C7−C8 bond by ∼37° (Figure 1a) in the triplet state. This type of orientation change between the ring and attached carbonyl group has been predicted for several simple aromatic carbonyl compounds in previous work using singlet−triplet-state absorption and phosphorescence measurements.[29−31,33] Our results show an analogous variation in this regard for HPDP. The ring connected carbonyl group twists out of the ring plane by ∼21° in the triplet state vs ∼2° in the ground state and the rotation about the C11−C10 (Figure 1b) bond induces a substantial change in the relative orientation between the *p*-hydroxyphenacyl moiety and the leaving group. The carbonyl carbon atom maintains its sp^2 character in both the triplet and ground states as indicated by the ∼360° sum of angles around it (C7 in HA and C11 in HPDP).

Bond lengths also vary substantially on going from the ground state to the triplet state. For both HA and HPDP, the ring center C−C bond shows some shortening (by ∼0.01 Å) but the shoulder C−C band near the carbonyl substituent lengthens by ∼0.03 Å, and the carbonyl C−O bond increases greatly by ∼0.1 Å. The C−C bond connecting the ring and carbonyl group shortens extensively by ∼0.08 and ∼0.06 Å, respectively, for HA (C4−C7) and HPDP (C13−C11), and the nearby C−C bond length, C7−C8 in HA and C11−C10 in HPDP, becomes reduced by 0.02 and 0.04 Å, respectively, in the triplet state. For HPDP, the bond length of the C−O bond connecting the *p*-hydroxyphenacyl and the leaving group (C10−O5) increases by ∼0.04 Å in the triplet state compared to the ground state, but the structural parameters related to

the phosphate leaving subgroup remain almost unchanged in the triplet state and the ground state.

The structural changes in the triplet state compared to the ground state are consistent with the associated frequency variations on going from the ground to triplet states for both HA and HPDP. For example, the slight bond length change for the ring center C−C bond is consistent with the observation that the mode dominated by stretching of this bond (the Wilson 8a band) shows little frequency change in the triplet state (1599 and 1612 cm^{-1} for HA and HPDP, respectively) compared to its ground-state values (1596 and 1609 cm^{-1} for HA and HPDP, respectively). Similarly, the significant shortening of the C−C bond joining the ring and carbonyl group is in line with the frequency increase for the mode contributed most by the stretching of this bond that have been identified at 1378 and 1371 cm^{-1}, respectively, for the triplet states of HA and HPDP compared to 1235 and 1237 cm^{-1}, respectively, for the HA and HPDP ground state. The bond length and stretching frequency of this bond indicate that the bond gains significant double-bond character in the triplet state. This suggests that the calculated structures and the preliminary vibrational assignments made based on the calculations are reasonable and can provide a valid interpretation of the experimental spectroscopic observations detailed here.

The carbonyl C−O stretching mode deserves a special comment due to its essential role in the nature and properties of the triplet states for aromatic carbonyl compounds. As illustrated previously, our results show that there is no localized C−O stretching mode in the triplet states for both HA and HPDP. The only possible band with a noticeable contribution from the C−O stretching has been found, according to the DFT calculations, at 1257 cm^{-1} for both HA and HPDP (Tables 3S and 4S, Supporting Information). Compared with the localized C−O stretching frequency in the ground state (1654 and 1660 cm^{-1} for HA and HPDP, respectively), this corresponds to a ∼400 cm^{-1} downfield shift for the triplet state, indicating a striking weakening of this bond in the triplet state compared to the ground state. This is in good agreement with the calculated 0.1 Å increase of the C−O bond length on going from the ground state to the triplet state. We note that the triplet state C−O bond length (1.317 and 1.314 Å for HA and HPDP, respectively) becomes parallel to the single C−O bond length connecting the ring and hydroxyl group (C1−O1 length of 1.359 Å in HA and C16−O19 length of 1.358 Å in HPDP). This implies single-bond character for the carbonyl group in the triplet state as compared with the typical double C═O bond in the ground state.

According to the results of the DFT molecular orbital (MO) calculations for both HA and HPDP on going from the ground state to the triplet state, the above mentioned structural and vibrational changes are due to an electron excitation from the highest occupied π bonding orbital to the lowest unoccupied π^* orbital. The bonding π orbital resides mainly on the ring shoulder C−C bonds, while the π^* orbital contributes to both the ring and carbonyl orbitals with some π-bonding character for the C−C bond connecting the two parts. The DFT calculations find a similar $\pi\pi^*$ transition character for the HPDP triplet state. This $\pi\pi^*$ transition therefore causes a reduction in the electron density for the ring and carbonyl portions of the molecule but an increase of the electron density for the connecting C−C bond. This presents an explanation for the frequency shifts and geometric changes for the corresponding subgroups in the triplet state relative to the ground state.

On the basis of the studies of the triplet-state lifetime, the reactivity of the triplet state toward hydrogen atom abstraction reactions, and the shape and position of the phosphorescence spectrum, it has been concluded previously that the triplet state of HA is $\pi\pi^*$ in nature.[17,33] Our results are consistent with this. However, we note that our results regarding the carbonyl configuration are not quite in line with the earlier suggested correlation between the triplet state nature and the carbonyl C−O stretching frequency. Previous TR[3] and TRIR work found that the frequency of the C−O stretching appears in the 1500−1600 cm^{-1} range for typical $\pi\pi^*$ triplet states and in the 1200−1400 cm^{-1} region for nπ^* nature triplet states.[34−36,38,39,73] Examples of the former case are the 1522, 1600, and 1542 cm^{-1} C−O stretching frequencies for the triplet states of 4-phenylbenzophenone,[34,73] fluorenone,[38] and duroquinone,[40] respectively, and an example for the latter case is the 1222 cm^{-1} C−O frequency for the benzophenone triplet state.[35,36] These studies concluded that the carbonyl C−O bond retains its double-bond character for the $\pi\pi^*$ triplet state but gains single-bond character for the nπ^* triplet state. Based on this correlation, the $\pi\pi^*$ triplet states of HA and HPDP will be predicted to have a double bonded carbonyl group, rather than a nearly single C−O bond, as discussed here. This discrepancy must stem from a fundamental difference in the electronic properties of the compounds studied here and those examined in the previous investigations and can be understood in the following manner.

It has been quite clear that for aromatic carbonyl compounds the pure nπ^* excitation leads to an electronic transition localized on the carbonyl group, while the pure $\pi\pi^*$ transition induces changes in the electron distribution localized on the ring sub-group.[17,28,33,55,56] The frequency of the observed vibrational bands such as the C−O stretching band is a reflection of the associated bond order and is related to the electron-overlap population for the correspond bond. In this sense, it is reasonable to expect that the C−O bond will become single bond-like and the C−O frequency appears in the single bond C−O stretching region for a nπ^* triplet state whereas it retains the double-bond character for a $\pi\pi^*$ triplet state. This justifies the correlation of the C−O stretching frequency with the triplet state nature proposed in the earlier studies.[34−36,38,39,73] As manifested by the absorption and phosphorescence measurements, the nπ^* and $\pi\pi^*$ levels are found to be well-separated for the above-mentioned aromatic carbonyl compounds examined in the previous vibrational spectroscopic studies and the triplet states of these compounds have been established to be predominately nπ^* or $\pi\pi^*$ in nature, though not pure nπ^* or $\pi\pi^*$ in character.[17,31,33,74,75]

However, when the two configurations are close in energy or almost isoenergetic, as in the case of acetophenone and its derivatives, the properties of the triplet states cannot be described by this simple interpretation and have been found to be highly sensitive to modest perturbations. For example, the type and position of the ring substituent group, the temperature, the polarity, or

the hydrogen-bonding strength of solvent environment, etc. can induce noticeable changes. Extensive spectroscopic studies have been performed to seek a link between the nature of the triplet state and the substituent or solvent effects for these compounds.[17,20,22,28−31,33] It has been established that the extent of electronic and vibrational mixing between the nearby nπ^* and $\pi\pi^*$ triplet states are among the major factors to account for the observed complicated spectroscopic characteristics and the widely different triplet-state reactivity.[17,20,22,28−31,33] In the case of HA and HPDP, the presence of the *para*-electron donating −OH group leads to an energy increase for the ring π orbital and subsequently causes (i) a lowering of energy for the $\pi\pi^*$ transition relative to the nπ^* transition and (ii) a change in the extent of conjugation between the ring π system and the carbonyl π orbital.[17,28,30,33] This accounts for (i) the reversion of the triplet state from nπ^* in acetophenone to $\pi\pi^*$ in HA and (ii) delocalization of the π conjugation between the ring and carbonyl π system. Our DFT-calculated MO results indicate consistently that the half-occupied π^* orbital has a significant component from the carbonyl π^* contribution. By showing that the free spin density distributes mainly on the carbonyl carbon and oxygen atoms, with some appreciable amount distributed on the three-ring carbon atoms (see Table 2), our calculated results for the spin density also supports the delocalization of the π system for the $\pi\pi^*$ triplet states of HA and HPDP. The increased conjugation is thus responsible for the substantial weakening of the C−O bond and the considerable strengthening of the ring-carbonyl between C−C bond in the triplet state compared with the ground state. A large change in the C−O force constant for the $\pi\pi^*$ triplet state compared with the ground state has been reported in previous studies for some closely related aromatic carbonyl compounds.[31,33] Since the extent of this conjugation could be different for the wide variety of acetophenone derivatives with substituents of different electron donating ability, it is reasonable to infer that there could be no general applicable description for the C−O bonding character in the $\pi\pi^*$ triplet state. It is probable that the C−O bond could be double bond-like for the ring localized $\pi\pi^*$ triplet states but single bond-like for extensively delocalized $\pi\pi^*$ triplet states.

In the particular case of the C−O stretching mode, our results suggest that there is no such localized mode for the triplet states of HA and HPDP. A similar conclusion has appeared in several earlier publications[31,33,37] and has been interpreted as being due to a decrease in the C−O frequency and a strong mixing of this mode with other vibrations of similar frequency so that the triplet state C−O stretching does not exist as a separate normal mode like that in the ground state. We note that, even for the compounds where the C−O mode was identified distinctly, the vibrational mixing of this mode with others has also been reported to be extensive.[34−36] This effect was taken to account for the observed extent of the carbonyl ^{18}O and ^{13}C isotopic shift. These shifts were observed to be noticeably smaller than those expected for a pure C−O stretching mode.

Vibrational coupling between the nearby nπ^* and $\pi\pi^*$ configurations has been established to be the other important factor in determining the triplet state structure for the acetophenone family of compounds. The torsional vibration of the $-C(O)CH_3$ group with respective to the ring plane and rotation of the $-CH_3$ group around the connecting C−C axis have been identified as effective out-of-plane modes to couple the two states for the acetophenone triplet states and this coupling was found to result in large conformational changes along the two coordinates for the triplet state structure.[29−31,33] Our results for the triplet state optimized structures shows that similar conformational changes also occur in the triplet states of HA and HPDP. For instance, for both the compounds, the carbonyl groups are found to be within or nearly within the ring plane in the ground state, but twisted out from the ring plane by ∼16° (HA) or 20° (HPDP) in the triplet state. In addition, the twisting was accompanied by the rotation around the C−C bond joining the carbonyl group and the nearby $-CH_2$ group. We therefore suggest that the vibrational coupling effects apply also for the triplet states of *p*-hydroxy-substituted acetophenone derivatives, though the energy gaps between the nπ^* and $\pi\pi^*$ are slightly wider in these compounds compared with that in acetophenone.[17,33]

In general, our results indicate that the triplet states of HA and HPDP are conjugated $\pi\pi^*$ in nature with a single bond like carbonyl group and a modestly twisted carbonyl structure. It appears that the previously proposed link between the carbonyl configuration and triplet-state nature is not applicable to the triplet states of these two compounds. We note that, besides the work reported here, there is little vibrational data available in the literature for the triplet states of aromatic carbonyl compounds with closely lying nπ^* and $\pi\pi^*$ configurations. Further accumulation of experimental vibrational frequency data for these compounds is highly desired in order to develop a more general understanding of the triplet state structure in terms of (i) the carbonyl-bonding character, (ii) the twisting conformation of the carbonyl group related to the ring plane, and (iii) and the extent of delocalization between the ring and carbonyl π systems. We feel that further investigations of this kind are also essential for seeking a comprehensive link between the structures and the wide range of the triplet state reactivity observed for aromatic carbonyl compounds.

F. Discussion Regarding the Initial Step of the Phenacyl Photodeprotection Reactions. The dynamics and structural information presented here for the triplet states of HA and HPDP have important implications in understanding the photodeprotection mechanism of the *p*-hydroxyphenacyl caged phototrigger compounds. To better address this point, we include the data reported here with our recent results for another *p*-hydroxyphenacyl caged compound, HPA (*p*-hydroxyphenacyl acetate).[16] Figure 10 displays a comparison between the triplet state resonance Raman spectra of HA, HPDP and HPA. It is obvious that the triplet state spectrum of HPA is almost identical to that of HPDP, and both are similar to HA triplet state spectrum. This corroborates the conclusion that the *p*-hydroxyphenacyl moiety is the chromophore responsible for the photoexcitation and Raman enhancement and that the triplet state structure is little affected by the existence and the type of leaving group. Under nitrogen purge conditions, the triplet state lifetime of HPA was found to be ∼137 ns, similar to that

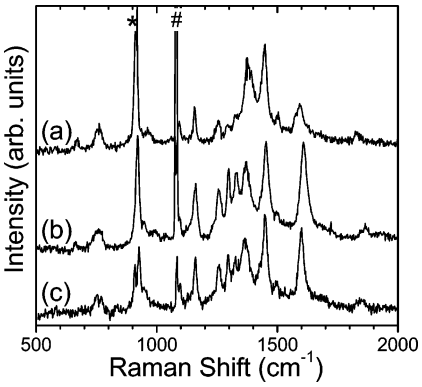

FIGURE 10. Comparison of the triplet state spectra of HA, HPDP and HPA obtained using nanosecond time-resolved resonance Raman spectroscopy with 266 nm pump and 416 nm probe wavelengths. The asterisks (∗) mark solvent subtraction artifacts. The # band is due to stray laser line.

of HPDP (150 ns) but longer than the HA triplet state lifetime (86 ps). The longer triplet state lifetimes for HPDP and HPA imply faster triplet state deactivation dynamics for HA than for HPDP and HPA. However, the ISC conversion was found to be equally rapid for HPA (less than 2 ps time constant) as for HA and HPDP.

In general, our work indicates unambiguously that photoexcitation of the *p*-hydroxyphenacyl caged compounds, including the parent compound HA, in acetonitrile solvent leads to solely photophysical processes, and a rapid generation of the triplet state by $\sim 5 \times 10^{11}$ s^{-1} ISC conversion from the excited singlet followed by nanosecond decay of the triplet state to the ground state. This result is in full agreement with the previous results from Givens and co-workers[6,7,9] and Wan and co-workers.[14] For HPA and HPDP as well as all *p*-hydroxyphenacyl caged compounds studied previously, the photoinduced cleavage and accompanying rearrangement reactions were found to take place only in water or in water mixed solvents. Although the work here was not done in a water involved environment, the $\sim 5 \times 10^{11}$ s^{-1} triplet state generation rate enables us to make comments regarding one of the major arguments about the phenacyl photodeprotection mechanism, that is, the issue of multiplicity. Givens and co-workers suggest that the photorelease occurs from the phenacyl triplet state,[6,7,9] whereas Wan and co-workers emphasized that the initial step is the excited-state intramolecular proton transfer (ESIPT) from the excited singlet state.[14] Our present result strongly favors that the triplet state is the transient precursor to the cleavage and related processes, although the detailed reaction pathway for the following steps has not been fully elucidated so far. This is further corroborated by the following issues: (i) To compete effectively with the $\sim 5 \times 10^{11}$ s^{-1} ISC conversion, the singlet state proton transfer proposed by Wan and coworkers must occur with a subpicosecond time constant. This is rather unlikely since the suggested proton-transfer mechanism is not a direct proton transfer between the donor and acceptor that may be reasonable to expect to occur on a subpicosecond or even femtosecond time scale.[18,76−81] It is a kind of water-mediated process between the well-space-separated proton donor (the −OH group) and acceptor (the carbonyl oxygen atom). It is conceivable that a suitably located and oriented water cluster composed of several water molecules may be required for such a mediated process to occur. Such a water cluster formation process necessitates translation and rotation of the water molecules, and this likely leads to the proton transfer to happen on a slower time scale and to subsequently not be efficient enough to compete with the very rapid ISC conversion. (ii) Transient absorption measurements for HPDP by Givens, Wirz, and coworkers found a sharp increase of the triplet state decay rate (with 400 ps time constant) in water/mixed acetonitrile (1:1 by volume) compared with that in pure acetonitrile solvent.[9] (iii) Preliminary ps-TR^3 measurements for HA, HPDP, and HPA in water/mixed acetonitrile (1:1 by volume) show that the early time development of the corresponding triplet state spectra are the same as those observed in neat acetonitrle, whereas the triplet state lifetimes become shortened differently for the three compounds in mixed water solvent compared to those in acetonitrle.[61]

We note, however, that the 267 nm excitation employed in the present work is at a shorter wavelength than those used in previous relevant studies that are typical above 300 nm.[6,8,10−12,14] As mentioned above, the 267 nm pump leads to instantaneous population of the S_3 state while the longer than 300 nm excitation populates mainly the S_1 state. Previous work finds that, for certain aromatic carbonyl compounds, the ISC rate and triplet yield can be affected substantially by the excitation wavelength.[43,82,83] It is thus necessary to consider the possible influence caused by this difference in the excitation in terms of the ISC process for the compounds studied here. Although the data presented provide no direct information for discussion of this issue, our very recent KTRF experiment on HP, HPDP, and HPA shows that, even with the 267 nm excitation, the ISC occurs from the S_1 state following the direct $^1n\pi^*$ $(S_1) \rightarrow {}^3\pi\pi^*$ (T_1) pathway and the ISC mechanism is the same in H_2O mixed (1:1 by volume) and neat acetonitrile with rather similar rate in both the solvents.[61] This implies that development of the triplet population does not depend on the excitation wavelength when the S_3 excitation introduces more excess energy into the system than S_1 excitation. We therefore believe that the photophysical and photochemical processes for HA and the *p*-hydroxyphenacyl caged compounds is not affected substantially by the excitation wavelength.

(74) Jones, P. F.; Calloway, A. R. *J. Am. Chem. Soc.* **1970**, *92*, 4997−4998.
(75) Ramseier, M.; Senn, P.; Wirz, J.*J. Phys. Chem. A* **2003**, *107*, 3305−3315.
(76) Organero, J. A.; Tormo, L.; Douhal, A. *Chem. Phys. Lett.* **2002**, *363*, 409−414.
(77) Ameer-Beg, S.; Ormson, S. M.; Brown, R. G.; Matousek, P.; Towrie, M.; Nibbering, E. T. J.; Foggi, P.; Neuwahl, F. V. R. *J. Phys. Chem. A* **2001**, *105*, 3709−3718.
(78) Folmer, D. E.; Wisniewski, E. S.; Stairs, J. R.; Castleman, A. W., Jr. *J. Phys. Chem. A.* **2000**, *104*, 10545−10549.
(79) Arzhantsev, S. Y.; Takeuchi, S.; Tahara, T. *Chem. Phys. Lett.* **2000**, *330*, 83−90.
(80) Lu, C.; Hsieh, R. M. R.; Lee, I. R.; Cheng, P. Y. *Chem. Phys. Lett.* **1999**, *310*, 102−110.
(81) Mukaihata, H.; Nakagawa, T.; Kohtani, S.; Itoh, M. *J. Am. Chem. Soc.* **1994**, *116*, 10612−10618.
(82) (a) Hirata, Y.; Lim, E. C. *J. Chem. Phys.* **1980**, *73*, 3804−3809. (b) Hirata, Y.; Lim, E. C. *J. Chem. Phys.* **1980**, *72*, 5505−5510.
(83) Ohshima, Y.; Fujii, T.; Fujita, T.; Inaba, D. *J. Phys. Chem. A* **2003**, *107*, 8851−8855.

An important observation related to the triplet state conformation that is helpful in better understanding the solvent dependence of the photorelease mechanism is that, upon going from the ground state to the triplet state, the structural and bonding changes for HPDP and HPA resemble those for HA in terms of the *p*-hydroxyphenacyl moiety. This together with the fact that the parent compound HA, bearing no leaving group, indicates that for the phenacyl caged compound, regardless of the kind of leaving group, the excitation energy is localized and lies predominately in the *p*-hydroxyphenacyl chromophore. This implies that after generation of the triplet state, further processes, most likely triplet state deprotonation and/or protonation reactions[42,75,84−86] and solvation of leaving group,[44,87] are required to induce an energy or/and charge redistribution between the phenacyl cage and the leaving group and consequently trigger the photodeprotection and rearrangement to occur. In this regard, our results provide an explanation to the experimental observation that the photorelease reaction does not happen in accetonitrile solvent, where only the triplet state is formed. This, on the other hand, implies that water, as a solvent and likely participant, must play a crucial role in the cleavage related processes.

For HPDP and HPA, the structural and bonding changes associated with the leaving groups in the triplet states compared with ground states are speculated to bear information regarding the photorelease pathway for the phenacyl caged compounds. Such conformational changes includes (i) a variation of the relative orientation between the leaving groups and the phenacyl subgroup and (ii) a small but noticeable lengthening (by ∼0.04 Å) of the C−O bond joining the phenacyl and leaving group. The extent of these changes is comparable in HPA and HPDP. Although the slight lengthening of the C−O bond appears to favor a direct cleavage of this bond being responsible for release of the leaving group, its small extent is not convincing enough to lend a solid support to this argument. This is especially true when taking into account that the extent of the lengthening is almost identical for HPA and HPDP, whereas the photorelease rate is much faster for HPDP than HPA.[7,14,61] Furthermore, the relative orientational change of the leaving group to the phencyl cage seems to be caused by rotation of the carbonyl connecting −C(O)-CH_2- bond, with not much relevance to the cleavage step. However, at the present stage, we cannot rule out completely the direct cleavage pathway proposed by Givens and Wirz.[6,9−11]

The $\pi\pi^*$ nature triplet state of the phenacyl compounds and lack of the triplet state reactivity toward hydrogen atom abstraction implies this pathway is not applicable to the *p*-hydroxyphenacyl system, although it has been shown to account for photorelease of unsubstituted phenacyl caged compounds.[15]

Plausible mechanisms for the water-assisted cleavage pathways for the *p*-hydroxyphenacyl system could be (i) triplet-state protonation and/or deprotonation or (ii) water-catalyzed solvation of the leaving group to drive direct dissociation into ions. Regarding the first possibility, it is interesting to mention the well-established fact that phenols become stronger acids upon electronic excitation while aromatic ketones become stronger bases.[14,84−86] For HA, HPA, HPDP, and any other *p*-hydroxyphenacyl caged compounds with the two functional groups on the same chromophore, protonation at the carbonyl oxygen and/or deprotonation at the hydroxy site is highly likely to occur after photoexcitation. Such processes could possibly manifest themselves as the so-called formal intramolecular proton transfer but on the triplet state manifold due to the rapid ISC rate, rather than on the singlet manifold suggested by Wan and coworker.[14] These steps could lead to needed structural and electronic modification for the cleavage to occur. Regarding the second possibility, recent ps-TR^3 works by Kwok, Zhao, Phillips, and co-workers demonstrates that the water-catalyzed solvation of the leaving group is responsible for the decomposition of polyhalomethanes in water involved environments and this reaction pathway has been confirmed nicely by theoretical calculations.[44,87] It is possible that the *p*-hydroxyphenacyl caged compounds with different leaving groups depend on dynamic competition between the protonation/deprotonation and water solvation of the leaving group or that the photorelease processes follow a different pathway and mechanism. Further ps-TR^3 experiments involving changing the nature of the leaving group, the water concentration in the mixed solvent, the pH value of the solvent, etc., should prove useful in better elucidating the overall mechanism for the deprotection reaction and relevant processes of *p*-hydroxyphenacyl caged compounds.

Conclusion

Picosecond and nanosecond TR^3 spectroscopy has been performed to study the structure and dynamics of the excited state of HA and the *p*-hydroxyphenacyl caged phototrigger compound HPDP in acetonitrile solvent. For both compounds, oxygen-sensitive intermediates have been detected and were attributed to $\pi\pi^*$ triplet states with estimated lifetimes of ∼40 and ∼150 ns for HA and HPDP, respectively. The ns-TR^3 measurements have also been done for HA-^{13}C and HA-D_4 to help aid the assignment of the triplet state carbonyl C−O stretching and the ring related vibrational modes. The triplet-state spectrum of HA and its spectral development at very early picosecond times were found to be quite similar to those of HPDP. We found that the triplet states are generated rapidly after photoexcitation (∼5×10^{11} s^{-1} ISC rate). Combined with the early time dynamics of the Raman bandwidth and frequency changes, we attributed the early picosecond spectral evolution to the combined consequences of the triplet state formation process and the relaxation of excess energy of the initially formed energetic triplet state produced from this rapid ISC conversion. These results favor that the triplet state is the precursor responsible for the photorelease and rearrangement processes of the *p*-hydroxyphenacyl caged compounds. DFT calculations were done for both the excited triplet states and singlet ground states in order to elucidate the structures and vibrational frequencies for the two compounds. The calculated spectra reproduce

(84) Peteanu, L. A.; Mathies, R. A. *J. Phys. Chem.* **1992**, *96*, 6910−6916.
(85) Bhasikuttan, A. C.; Singh, A. K.; Palit, D. K.; Sapre, A. V.; Mittal, J. P. *J. Phys. Chem. A* **1999**, *103*, 4703−4711.
(86) O'Leary, B. M.; Grotzfeld, R. M.; Rebek, J., Jr. *J. Am. Chem. Soc.* **1997**, *119*, 11701−11702.
(87) Kwok, W. M.; Zhao, C.; Guan, X.; Li, Y.-L.; Du, Y.; and Phillips, D. L. *J. Chem. Phys.* **2004**, *120*, 3323−3332.

the experimental spectra and the observed isotopic shifts for carbonyl ^{13}C and ring deuteration of HA reasonably well and were used to make tentative assignments to all the experimentally observed features. The observed frequency changes for the corresponding ground-state vibrational modes to those of the triplet state correlate with the calculated structural changes between the two states. For HPDP, the triplet state conformation of the *p*-hydroxyphenacyl moiety closely resembles the triplet state structure of HA. Comparison of the triplet state structures for HA, HPDP, and HPA with the corresponding ground state structures shows that the photoexcitation, and thus the induced conformational and bonding changes, are localized on the *p*-hydroxyphenacyl group, with the leaving groups little affected. This provides a possible explanation for the solvent dependent behavior of the phenacyl photorelease process. For both HA and HPDP, the major structural changes on going from the ground state to the triplet state are the significant lengthening of the carbonyl C−O bond and extensive shortening of the C−C bond connecting the ring and the carbonyl group. These changes are accompanied by the ring shoulder C−C bond becoming modestly longer and the center C−C bond becoming slightly shortened. The experimentally observed isotopic shifts, in conjunction with the DFT MO and spin density results, indicates that the triplet states of HA and HPDP can be described by a delocalized $\pi\pi^*$ transition with extensive conjugation between the ring and carbonyl π^* systems. There was no localized carbonyl C−O stretching mode observed for the triplet states of HA and HPDP. The slightly twisted carbonyl conformation in the triplet states was attributed to vibrational coupling of the closely lying $\pi\pi^*$ and $n\pi^*$ configurations. For HPDP, the C−O bond connecting the phenacyl and leaving group shows a modest lengthening in the triplet state, and due to rotation of the carbonyl connecting $C-CH_2$ group, the relative orientation of the phosphate leaving group with respect to the phenacyl group changes substantially in the triplet state from the ground state. However, further work is yet required to completely elucidate the cleavage pathway for phenacyl photodeprotection reactions.

Acknowledgment. The Research Grants Council of Hong Kong is acknowledged by D.L.P. (HKU 7108/02P and HKU 1/01C) and P.H.T. (HKU 7112/02P and HKU 7027/03P) for financial support. W.M.K. thanks the University of Hong Kong for the award of a Postdoctoral Fellowship.

Supporting Information Available: Table of vibrational frequencies, comparison of spectrum, and optimized structures and energies are provided. This material is available free of charge via the Internet at http://pubs.acs.org.

JO049331A